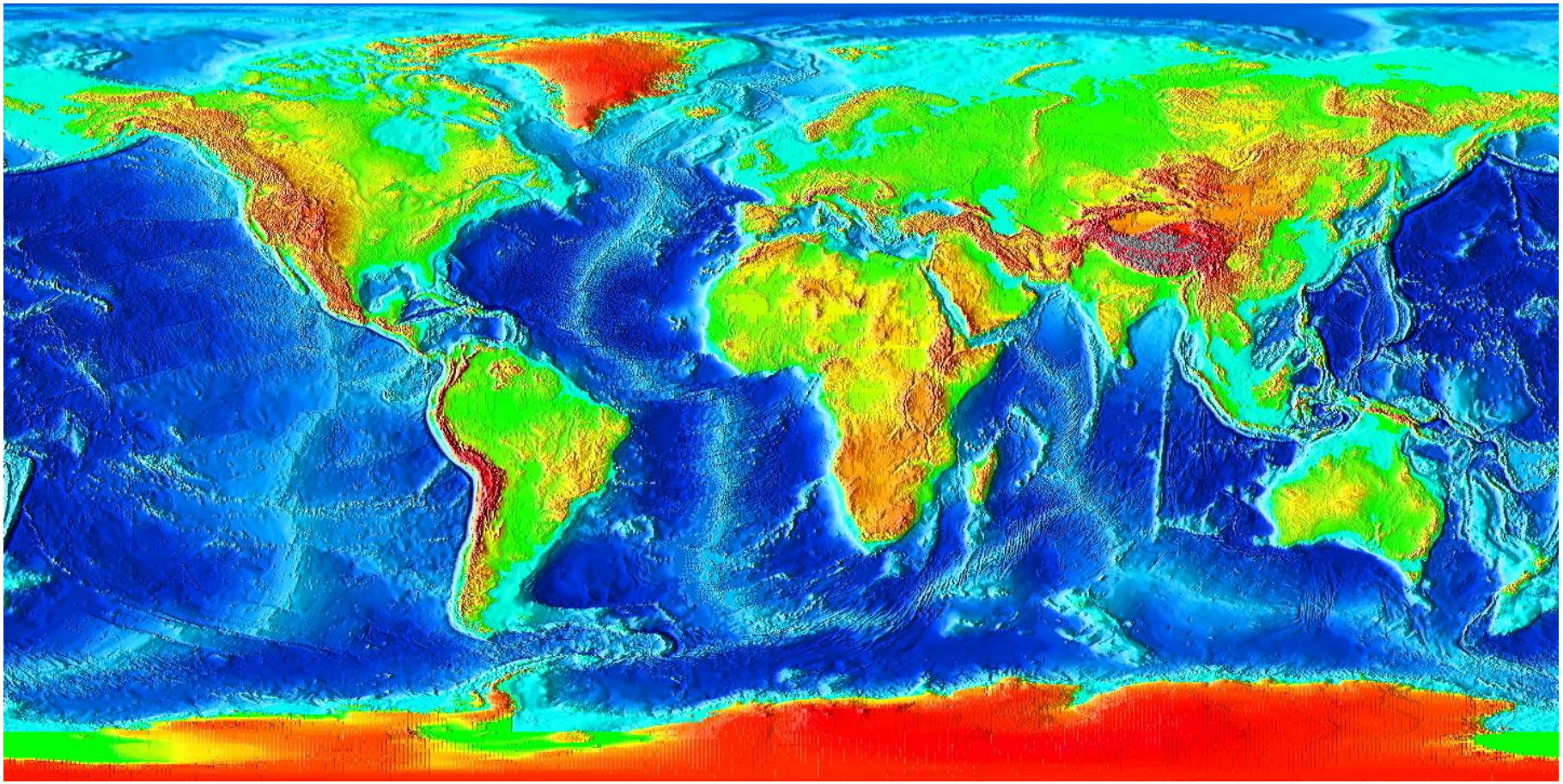

# crosta continental

Fábio R. D. de Andrade, Instituto de Geociências

USP Universidade de São Paulo
BRASIL

## crosta continental

41% da superfície terrestre
0,7% do volume terrestre
0,4% da massa terrestre

densidade média 2,7 a 2,9 g/cm$^3$

média de idade 2,0 a 2,3 Ga

porção quimica- e fisicamente mais complexa da Terra

espessura média 36km
entre ~20 km (zonas extensionais) e 100 km (zonas colisionais)

limite inferior – discontinidade sísmica de Mohorovicic

subdivisão crosta superior / inferior – discontinuidade física de Conrad (10-20km)

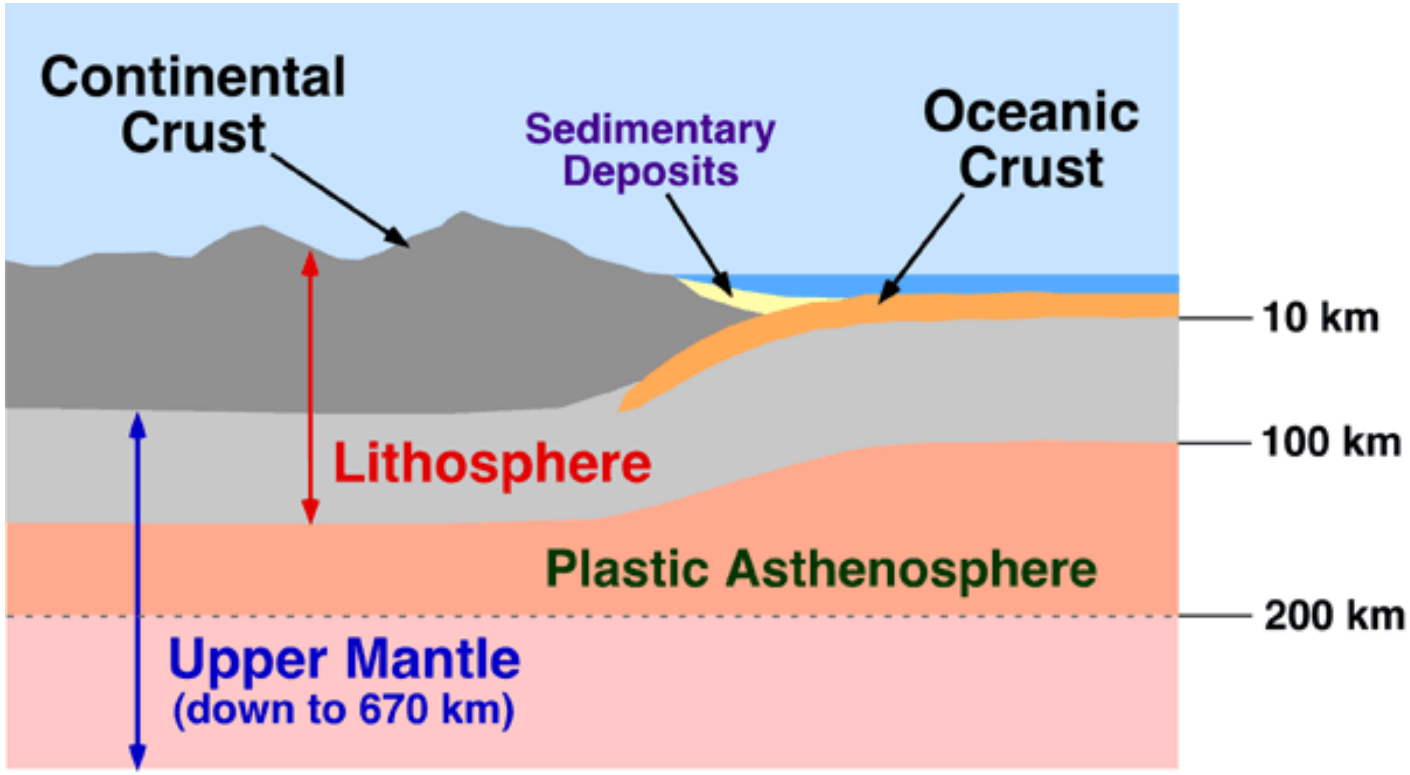
Continental Crust
Sedimentary Deposits
Oceanic Crust
10 km
100 km
Lithosphere
Plastic Asthenosphere
200 km
Upper Mantle
(down to 670 km)

as idades da crosta continental

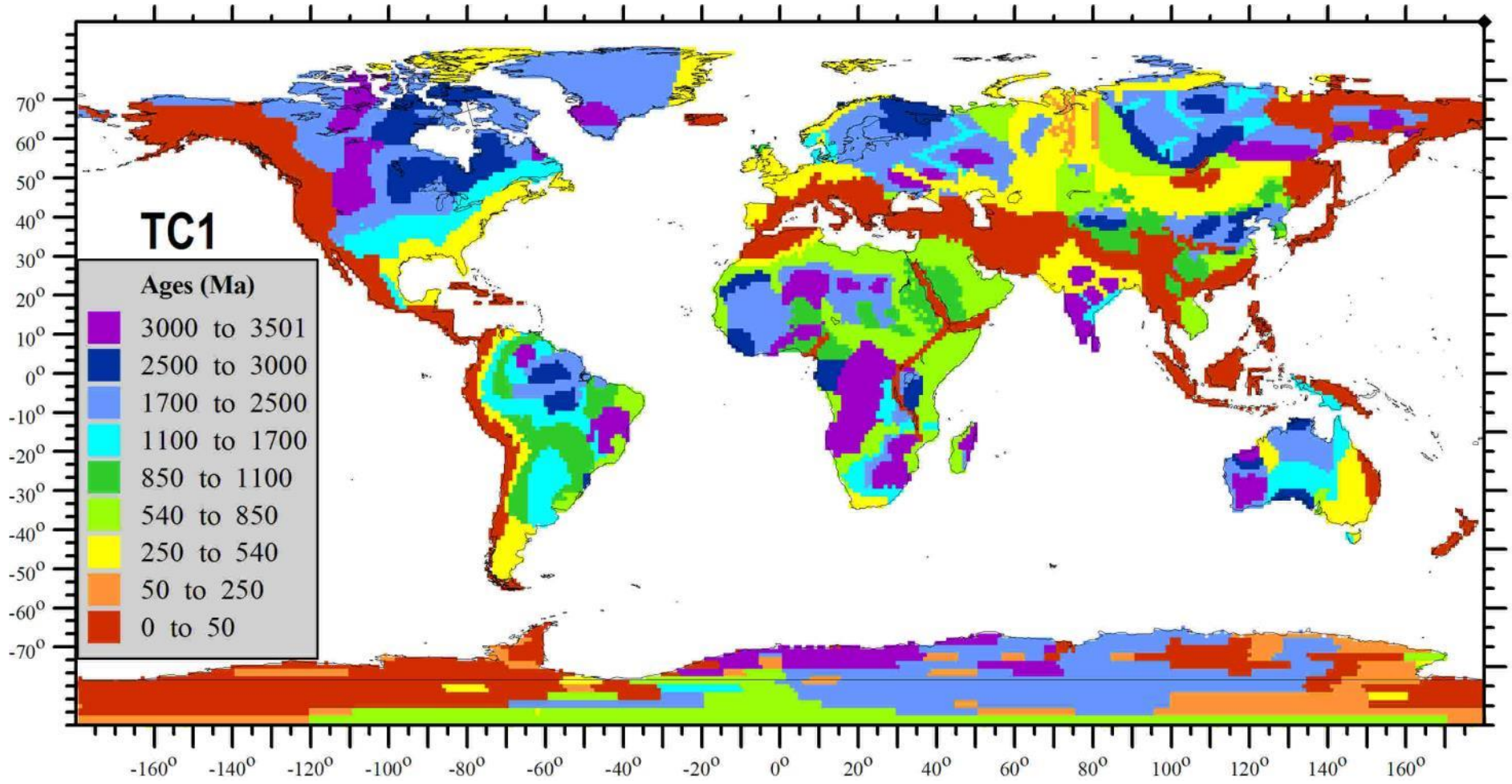


http://www.lithosphere.info/

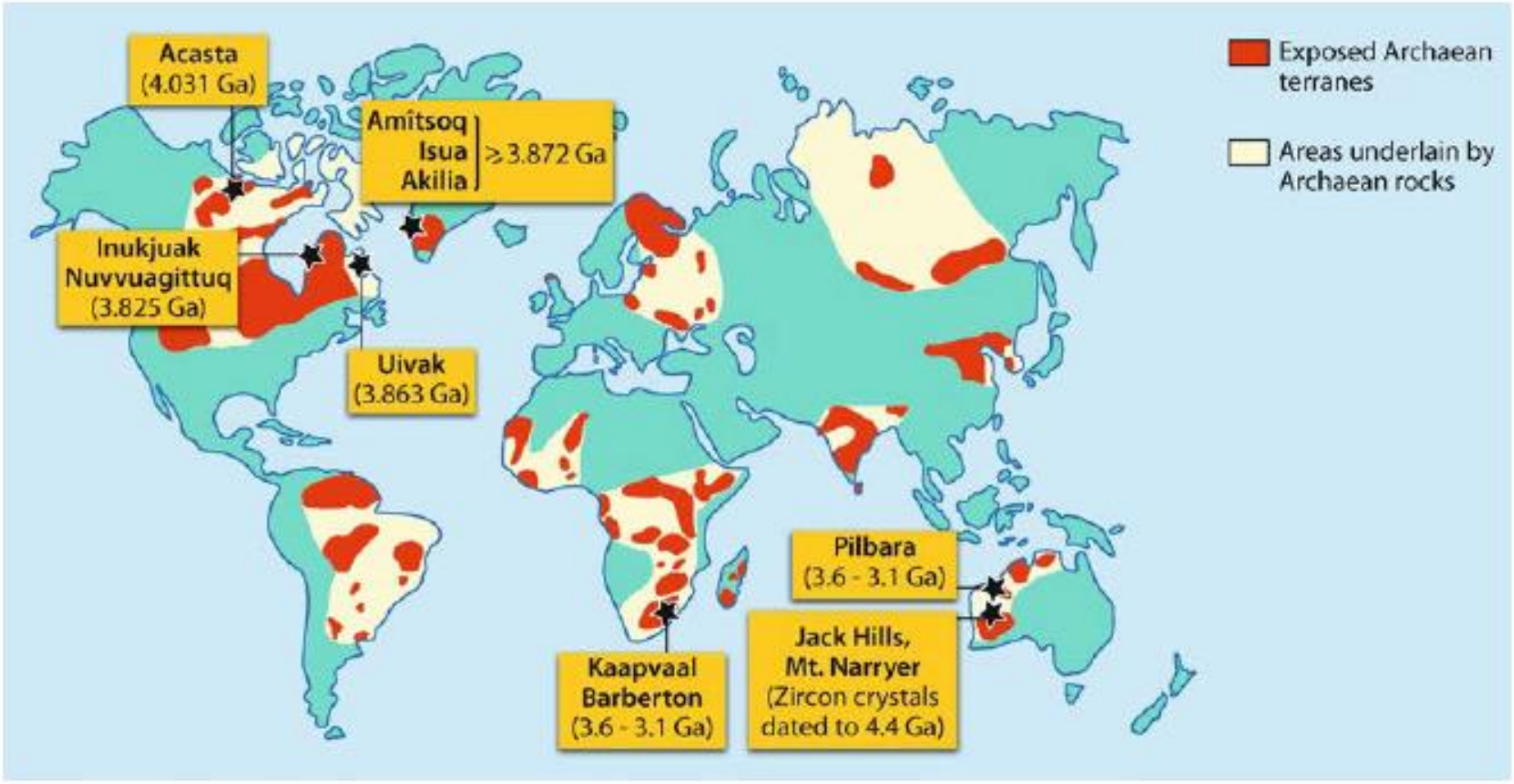


**Fig. 6.1 Simplified map of the Earth, showing the main outcrops of Archaean continental crust.** The oldest rocks known today are the Acasta gneisses; they are of magmatic origin and have a TTG composition (*see* p. 175). They outcrop over about 20 km² in the Northwest Territories in Canada. Slightly more recent, the Amîtsoq gneisses in Greenland and the Uivak gneisses in Labrador (Canada) are also ancient TTG. The oldest volcanic and sedimentary rocks catalogued today, crop out at Isua and Akilia (Greenland) as well as at Nuvvuagittuq (east Quebec). With surface areas of 1.2 and 0.06 million km², respectively, the Kaapvaal craton (South Africa and Swaziland) and the Pilbara craton (Australia) are the oldest Archaean terranes of continental size. Finally, it is worth remembering that the oldest terrestrial materials yet known as the zircon crystals discovered in Western Australia, at Jack Hills and at Mount Narryer (*see* ► Chap. 3).

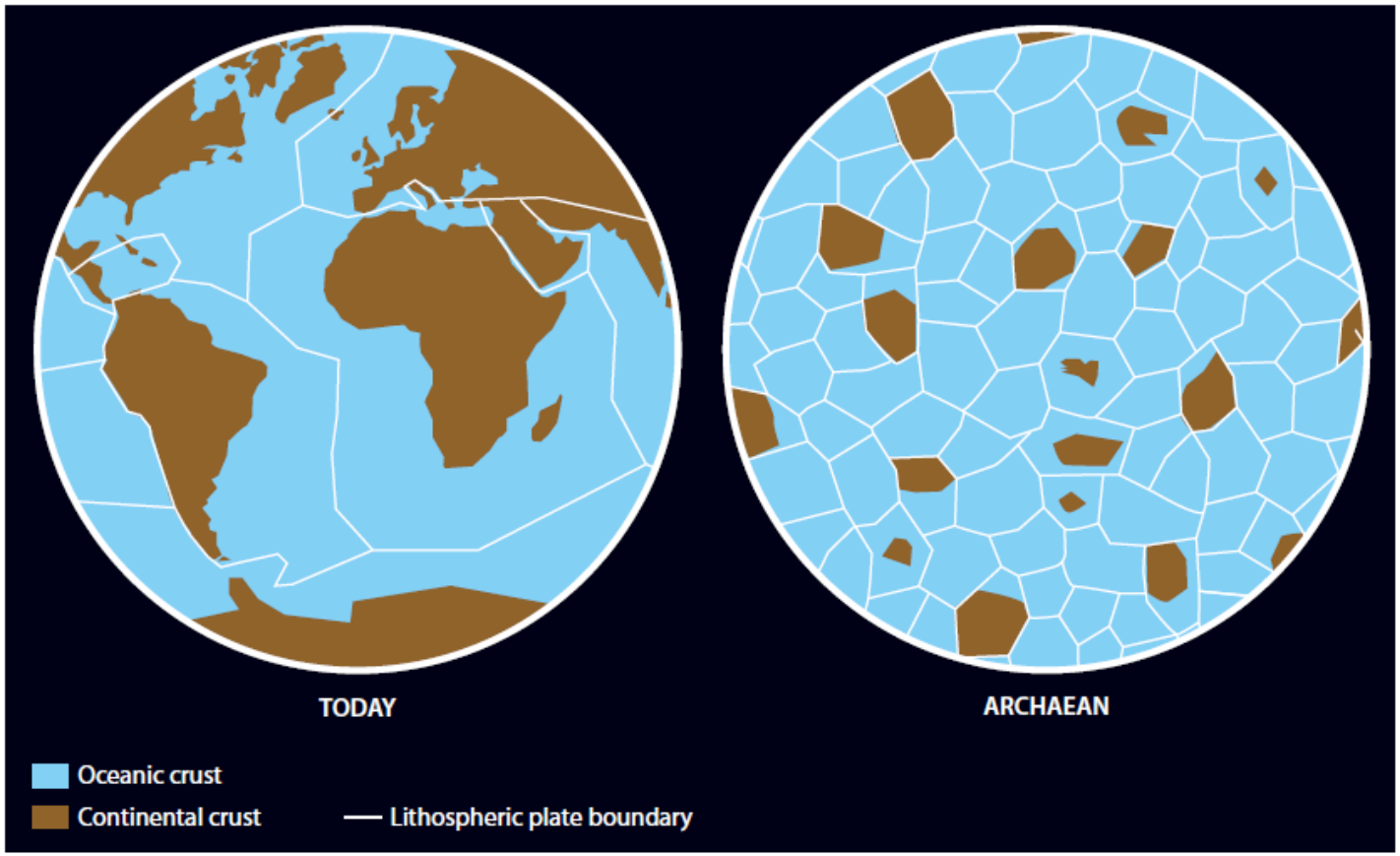


**Fig. 6.24 Comparison of the size of present-day lithospheric plates with the assumed size of Archaean lithospheric plates.** During the Archaean, Earth's internal heat production was greater than today. This heat was released through the mid-oceanic ridges, whose overall length, as a consequence, was also greater, which resulted in a mosaic of much smaller lithospheric plates than those found on the Earth today. (After De Wit and Hart, 1993.)

métodos de determinação da composição da crosta

Clarke

média de todas as análises disponíveis

Goldschmidt

análise de sedimentos finos de origem glacial (*loess*)

Taylor e McLennan

análise da composição de sedimentos fluviais (folhelhos)

razões entre elementos geoquimicamente semelhantes

correção considerando os elementos mais solúveis

Rudnick et al

modelos ponderados de dados geoquímicos e geofísicos

crosta oceânica *versus* crosta continental

| | basalto MORB |
|---|---|
| $SiO_2$ | 48,5 |
| $Al_2O_3$ | 15,0 |
| FeO | 11,8 |
| MgO | 11,0 |
| CaO | 11,4 |
| $TiO_2$ | 0,7 |
| $Na_2O$ | 1,5 |

*Brown e Musset (1995) Tab. 7.3 (p.123)*

| | Rudnick & Gao, 2003 |
|---|---|
| $SiO_2$ | 60.6 |
| $TiO_2$ | 0.7 |
| $Al_2O_3$ | 15.9 |
| $FeO_T$ | 6.7 |
| MnO | 0.10 |
| MgO | 4.7 |
| CaO | 6.4 |
| $Na_2O$ | 3.1 |
| $K_2O$ | 1.8 |
| $P_2O_5$ | 0.13 |
| Mg# | 55.3 |

# Composition of the Continental Crust

| | Rudnick & Gao, 2003 | Clarke* 1889 |
|---|---|---|
| $SiO_2$ | 60.6 | 60.2 |
| $TiO_2$ | 0.7 | 0.6 |
| $Al_2O_3$ | 15.9 | 15.3 |
| $FeO_T$ | 6.7 | 7.3 |
| MnO | 0.10 | 0.10 |
| MgO | 4.7 | 4.6 |
| CaO | 6.4 | 5.5 |
| $Na_2O$ | 3.1 | 3.3 |
| $K_2O$ | 1.8 | 3.0 |
| $P_2O_5$ | 0.13 | 0.23 |
| Mg# | 55.3 | 53.0 |

*F.W. Clarke, 1847-1931*

**Clarke, Frank Wigglesworth, for whom the Clarke medal is named*

http://geoscience.lngs.infn.it/Program/Pdf_presentations/Rudnick.pdf

# Composition of the Continental Crust

| | Christensen & Mooney 1995 | Rudnick & Fountain 1995 | Wedepohl 1995 | Taylor & McLennan 1985, 1995 | Rudnick & Gao, 2003 |
|---|---|---|---|---|---|
| $SiO_2$ | 62.4 | 60.1 | 62.8 | 57.1 | 60.6 |
| $Al_2O_3$ | 14.9 | 16.1 | 15.4 | 15.9 | 15.9 |
| $FeO_T$ | 6.9 | 6.7 | 5.7 | 9.1 | 6.7 |
| MgO | 3.1 | 4.5 | 3.8 | 5.3 | 4.7 |
| CaO | 5.8 | 6.5 | 5.6 | 7.4 | 6.4 |
| $Na_2O$ | 3.6 | 3.3 | 3.3 | 3.1 | 3.1 |
| $K_2O$ | 2.1 | 1.9 | 2.7 | 1.3* | 1.8 |
| Mg# | 44.8 | 54.3 | 54.3 | 50.9 | 55.3 |
| Th | | 5.6 | 8.5 | 3.5 | 5.6 |
| U | | 1.4 | 1.7 | 0.9 | 1.3 |

**Updated by McLennan and Taylor, 1996*

http://geoscience.lngs.infn.it/Program/Pdf_presentations/Rudnick.pdf

# Upper crust major elements: grid sampling

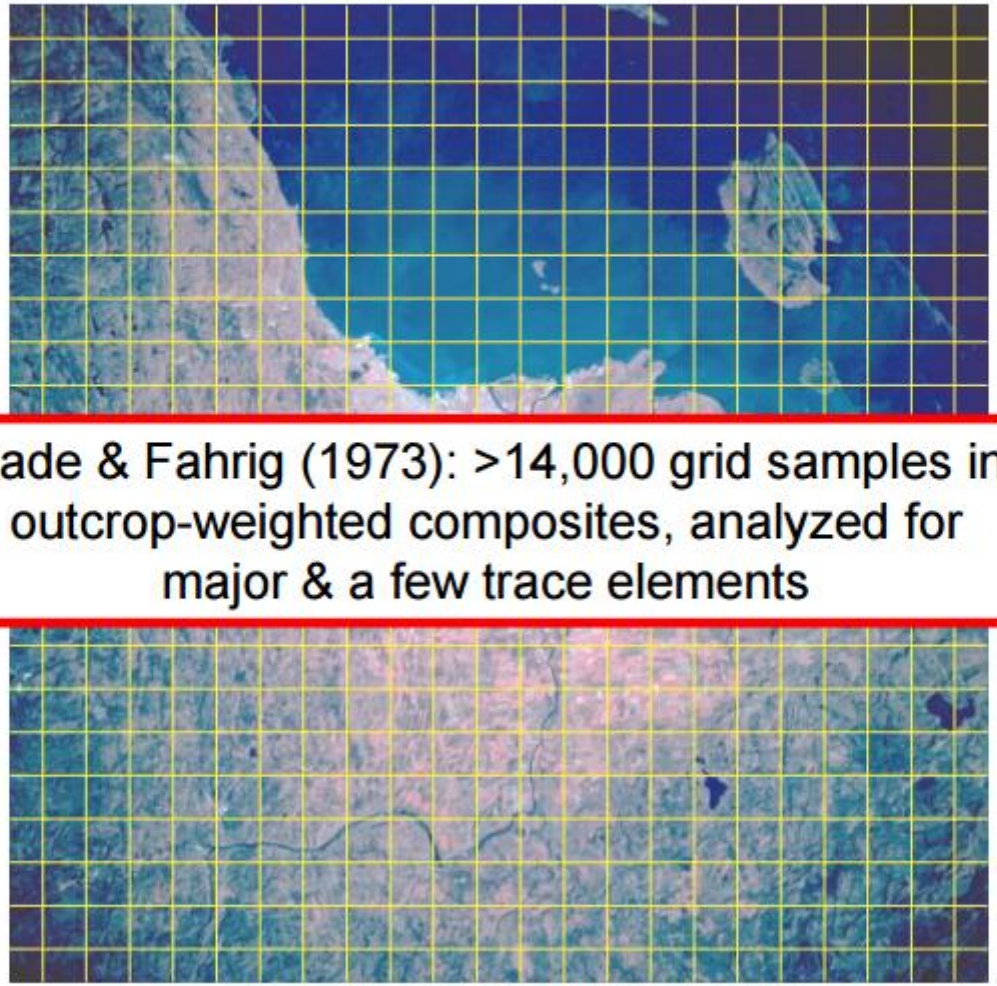

Eade & Fahrig (1973): >14,000 grid samples in outcrop-weighted composites, analyzed for major & a few trace elements

*Space shuttle view of Thunder Bay, Ontario*

# Upper crust major elements: Geological sampling

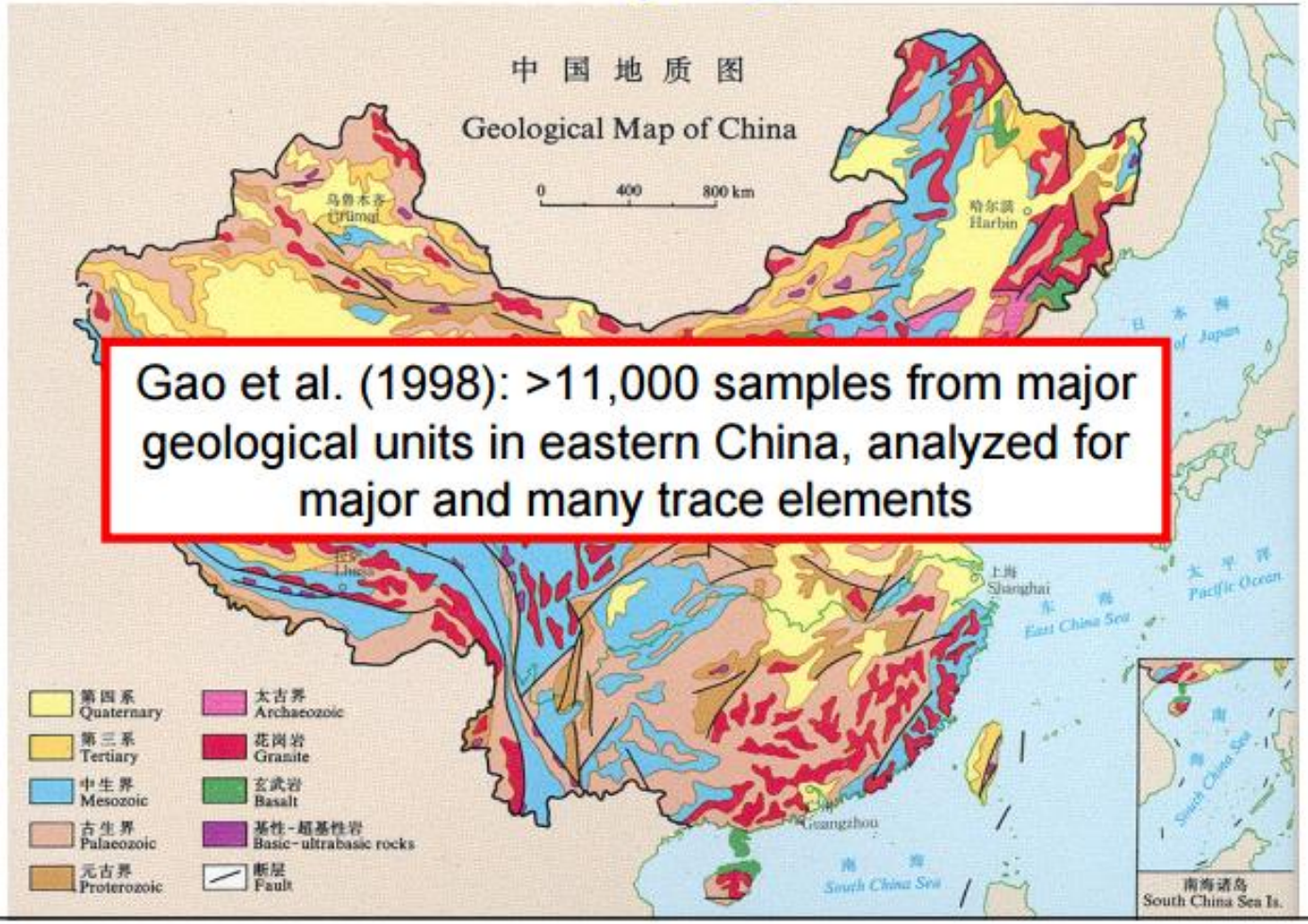

TABLE 1 Bulk compositional estimate of the continental crust

| | | | |
|---|---|---|---|
| $SiO_2$ | 59.1 | Ba | 390 |
| $TiO_2$ | 0.7 | La | 18 |
| $Al_2O_3$ | 15.8 | Ce | 42 |
| FeO* | 6.6 | Pr | 5.0 |
| MnO | 0.11 | Nd | 20 |
| MgO | 4.4 | Sm | 3.9 |
| CaO | 6.4 | Eu | 1.2 |
| $Na_2O$ | 3.2 | Gd | 3.6 |
| $K_2O$ | 1.9 | Tb | 0.56 |
| $P_2O_5$ | 0.2 | Dy | 3.5 |
| | | Ho | 0.76 |
| Mg# | 54.4 | Er | 2.2 |
| Li | 11 | Yb | 2.0 |
| Sc | 22 | Lu | 0.33 |
| V | 131 | Hf | 3.7 |
| Cr | 119 | Ta | 1.1 |
| Co | 25 | Pb | 12.6 |
| Ni | 51 | Th | 5.6 |
| Cu | 24 | U | 1.4 |
| Zn | 73 | K/U | 10,100 |
| Ga | 16 | Sr/Nd | 16 |
| Rb | 58 | La/Nb | 1.5 |
| Sr | 325 | Ce/Pb | 3.3 |
| Y | 20 | Nb/U | 8.6 |
| Zr | 123 | Th/U | 3.9 |
| Nb | 12 | Eu/Eu* | 0.96 |
| Cs | 2.6 | | |

These estimates are taken from ref. 37. Symbols used: Mg# = 100 × molar Mg/(Mg + $\sum$ Fe); FeO*, total Fe as FeO; Eu*, Eu value interpolated from REE pattern (see Fig. 4 legend).

Rudnick, 1995. Making continental crust, *Nature*, vol.378

velocidade das ondas sísmicas

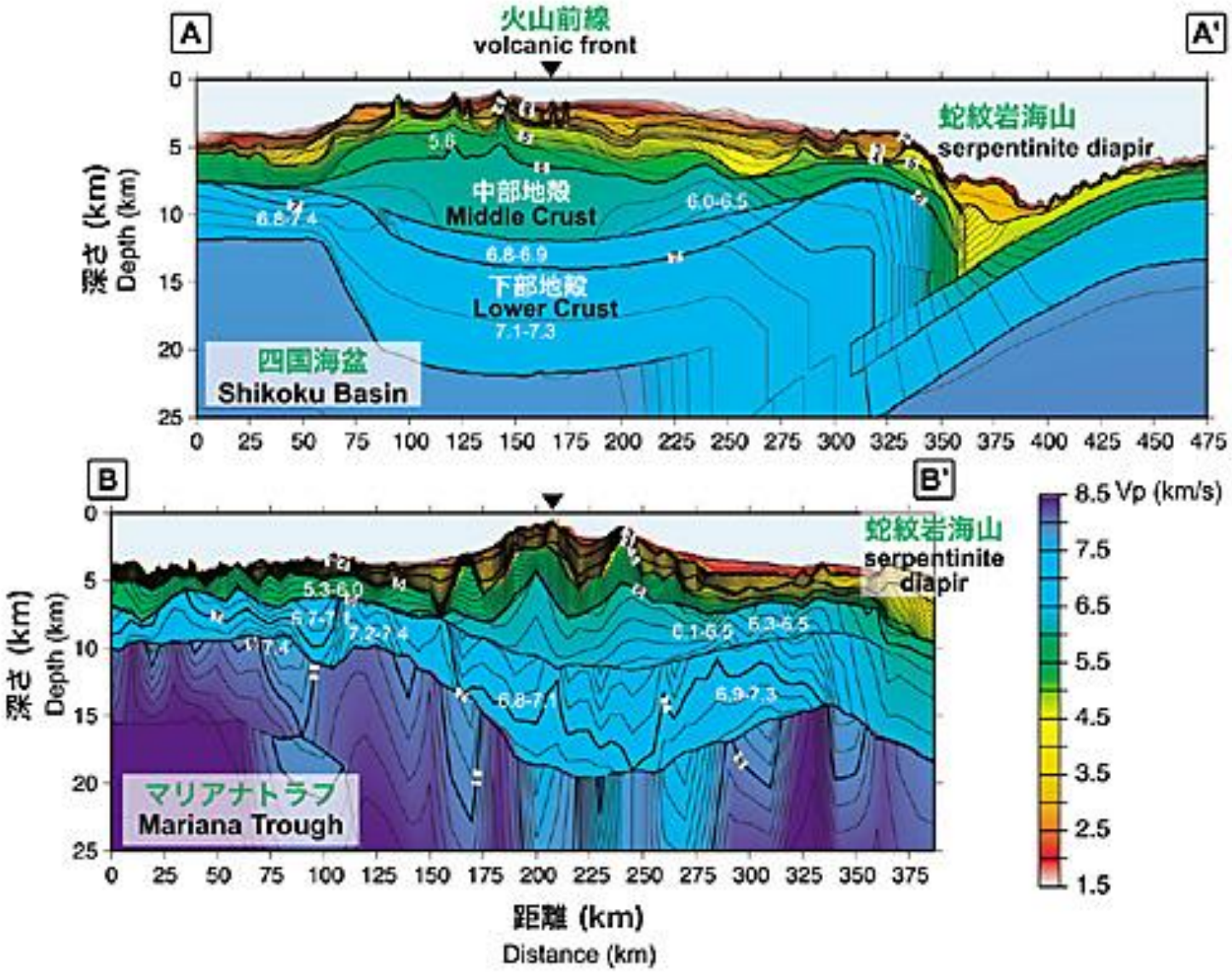


http://www.jamstec.go.jp/ifree/eng/03program/img/06/fig05.jpg

velocidade das ondas sísmicas

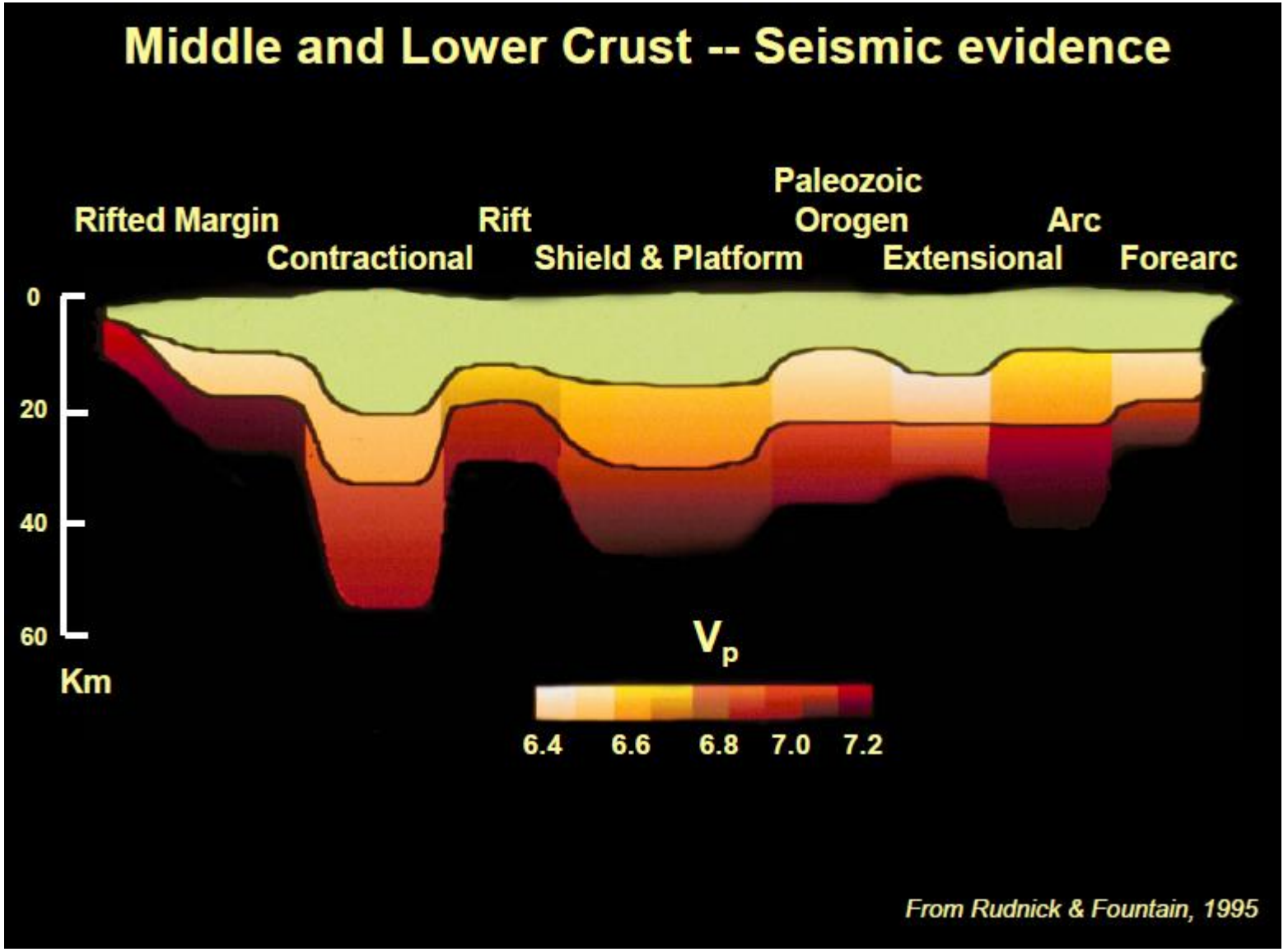

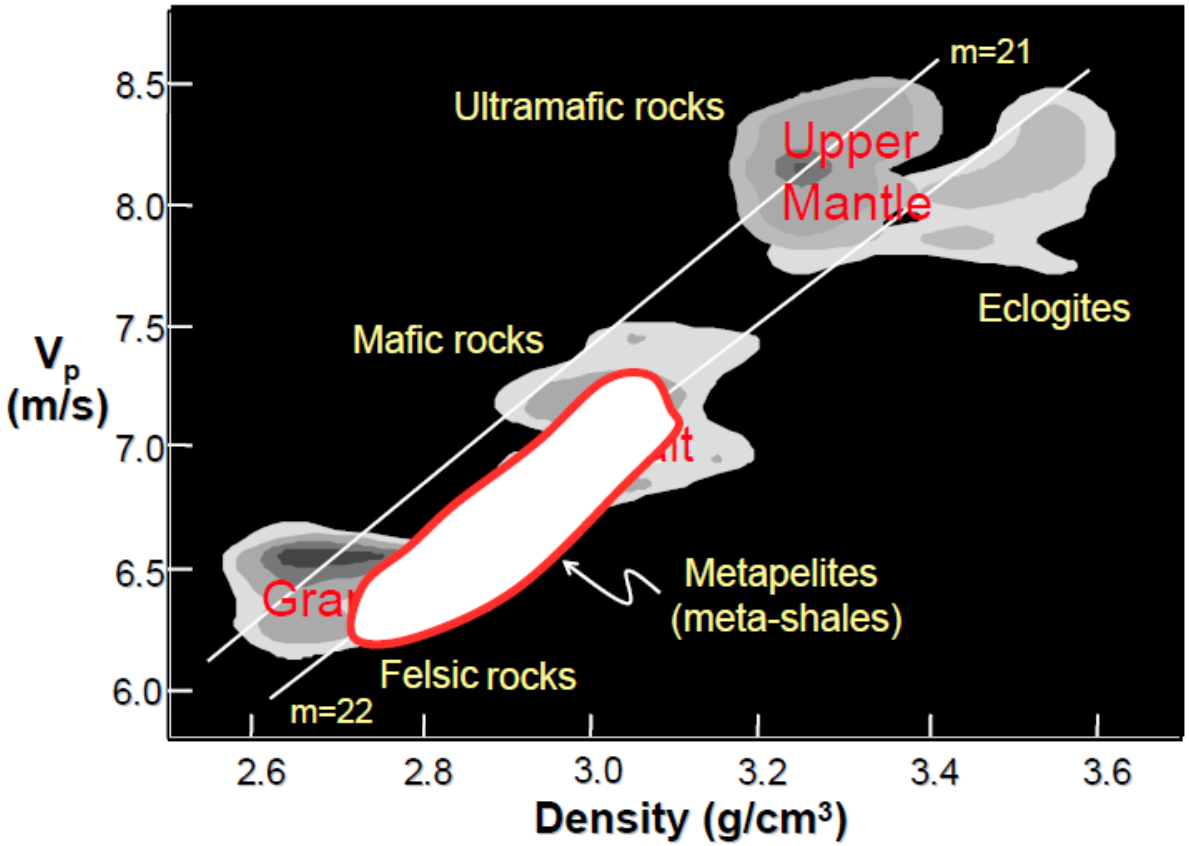


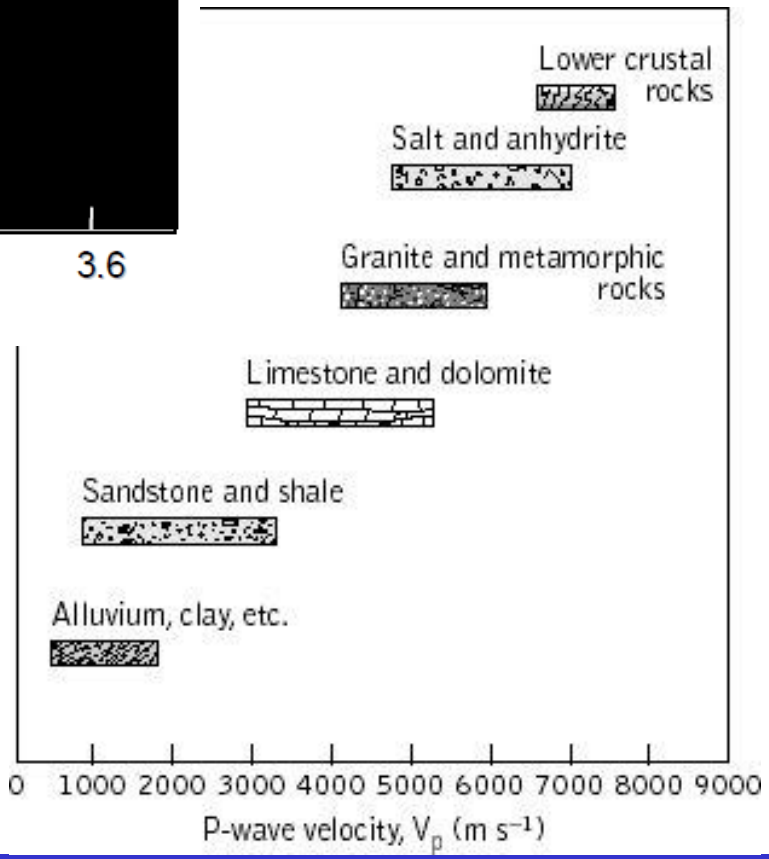


http://science.jrank.org/article_images/science.jrank.org/seismic-properties-of-rocks.1.jpg

crosta inferior
granulítica

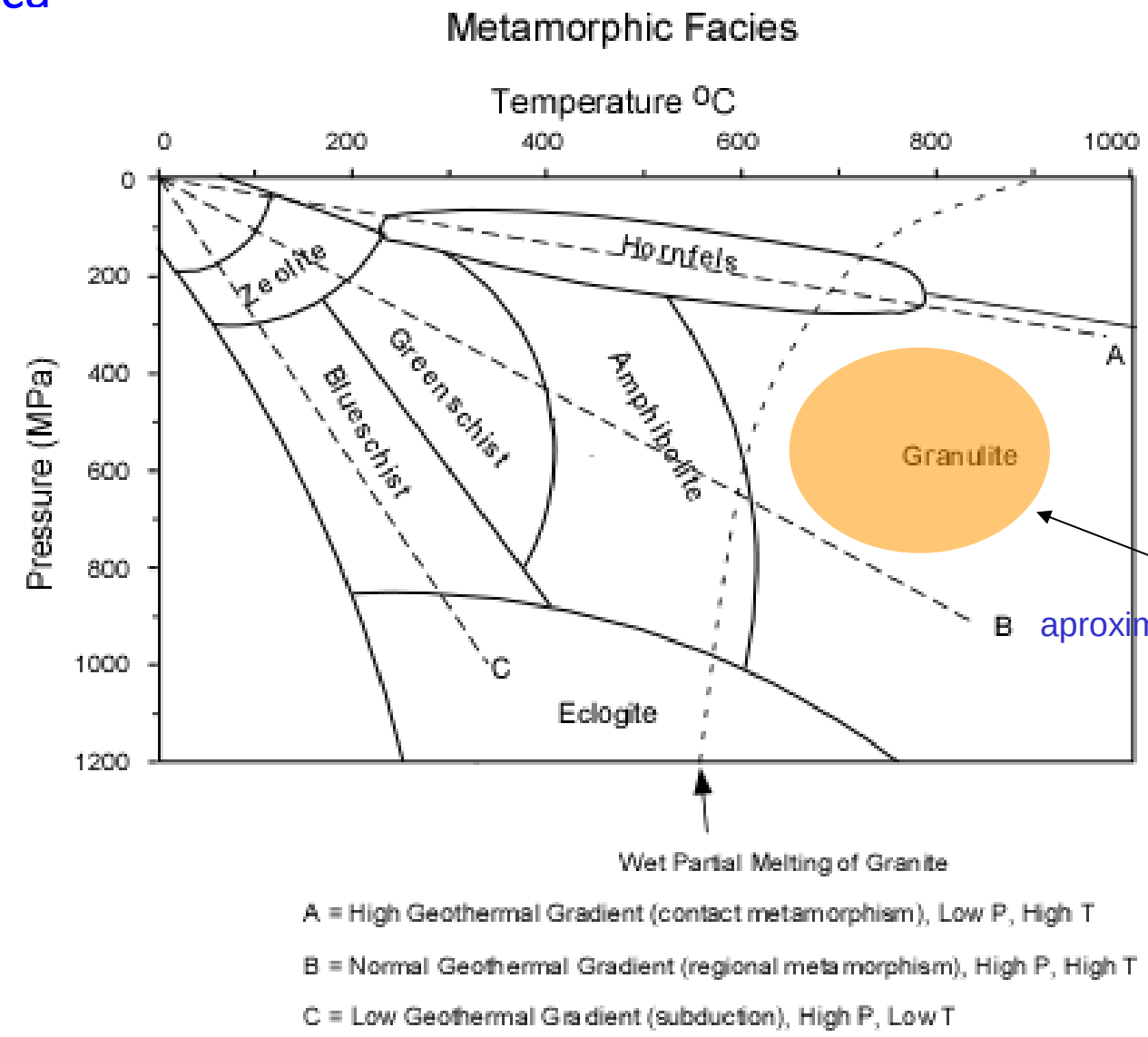


aproximadamente aqui

http://www.tulane.edu/~sanelson/eens212/metaclassification&facies.htm

# granulito

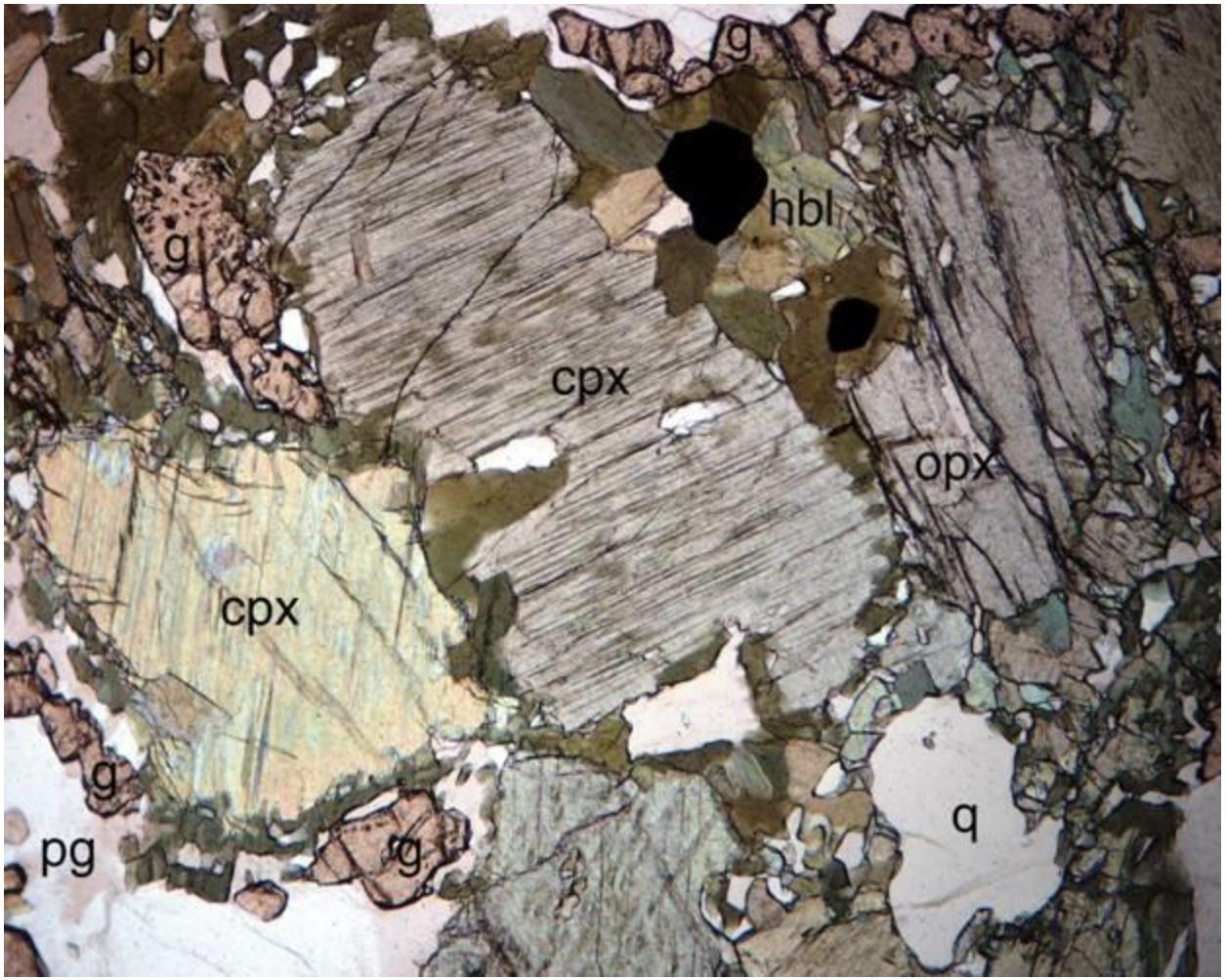


http://www.dukelabs.com/Abstracts%20and%20Papers/CMLO03TBMRates_files/image004.jpg

o termo granulito se refere a um fácies metamórfico
e não a uma composição química

granulitos...

...podem ser félsicos e máficos, refletindo a complexidade da crosta

...estão presentes nas crostas Arqueanas e Proterozóicas mais profundamente erodidas

...estão presentes em xenólitos de rochas vulcânicas

...estão de acordo com as velocidades sísmicas da crosta inferior

...são coerentes com a presença de granitos na crosta superior
(*magmas graníticos hidratados e resíduos anidros granulíticos*)

os granulitos são o resíduo de ciclos de fusão parcial que formaram a crosta superior

composição média da crosta superior

granodiorítica a tonalítica

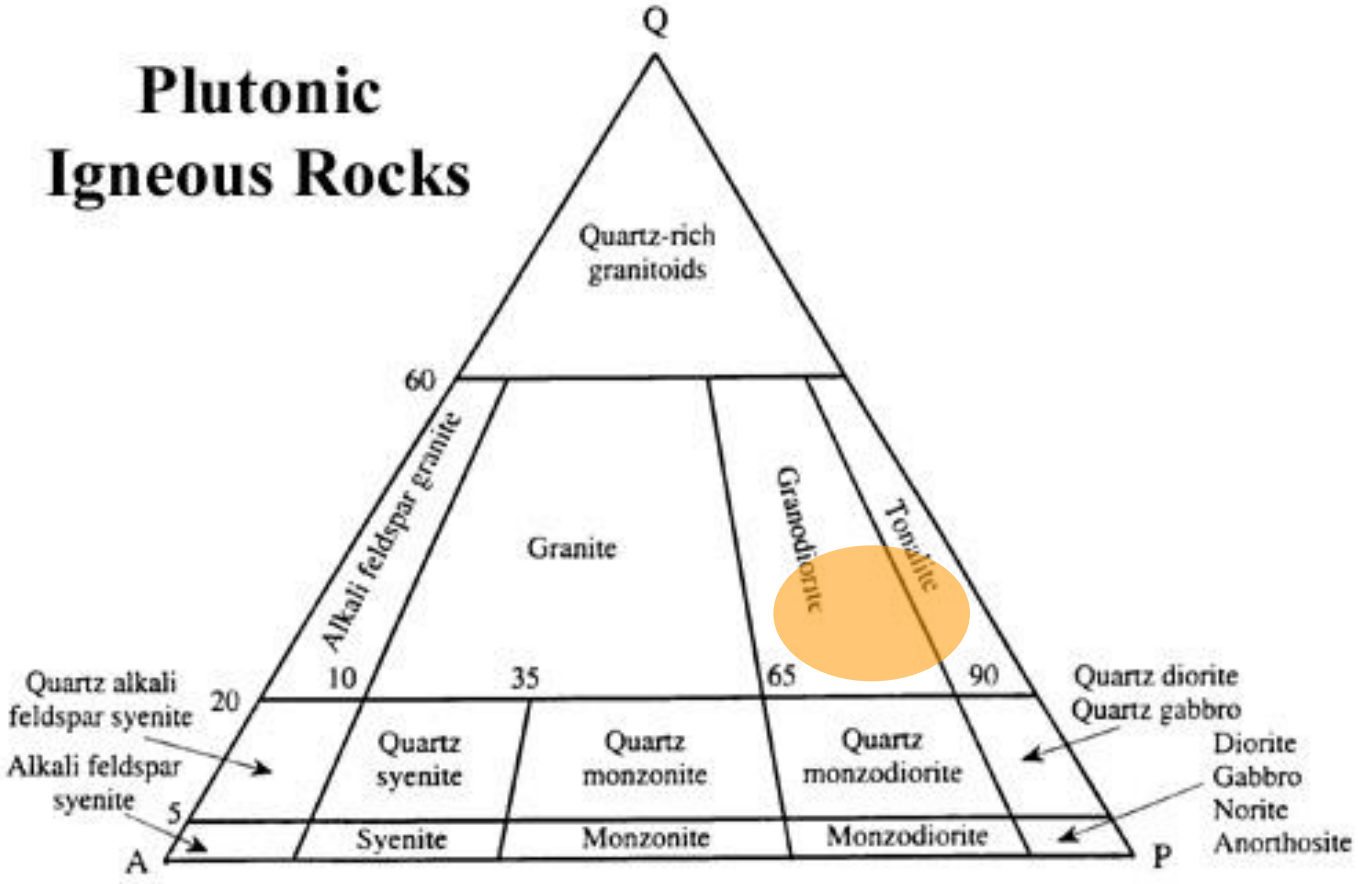

## crosta continental no Arqueano

grau geotérmico mais elevado

fusão da crosta oceânica subductada

formação de trondhjemitos (tonalito sódico)

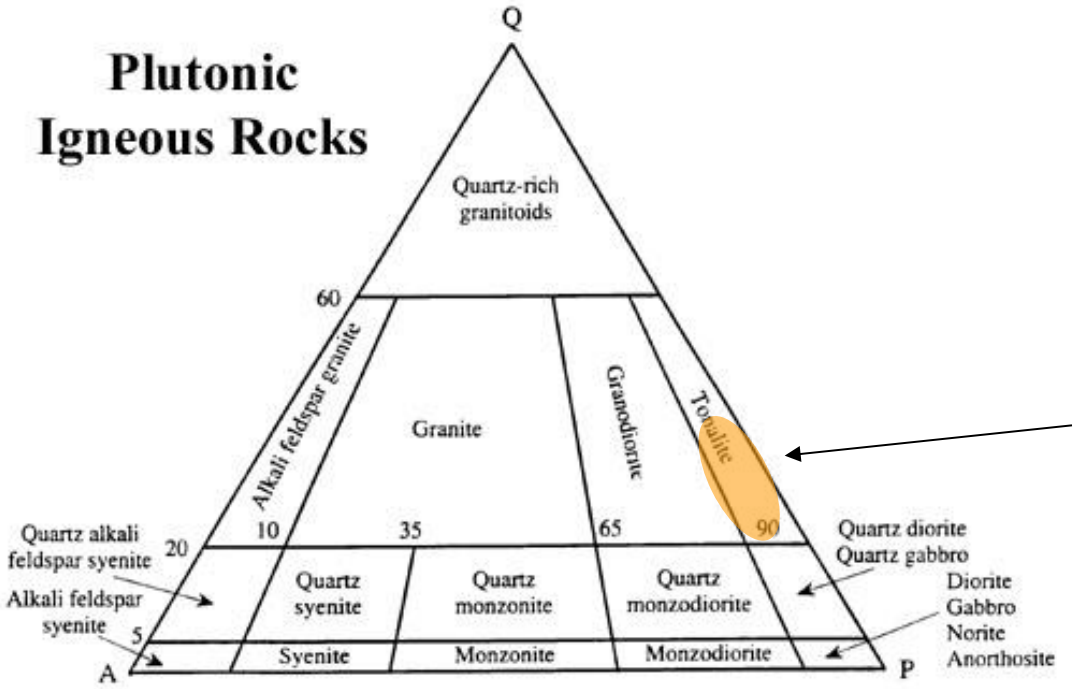


trondhjemito

http://folk.ntnu.no/krill/NTNU-geologi/prydsteinsveggen/120.jpg

## trondhjemito

granitóide composto por quartzo, plagioclásio sódico, máficos

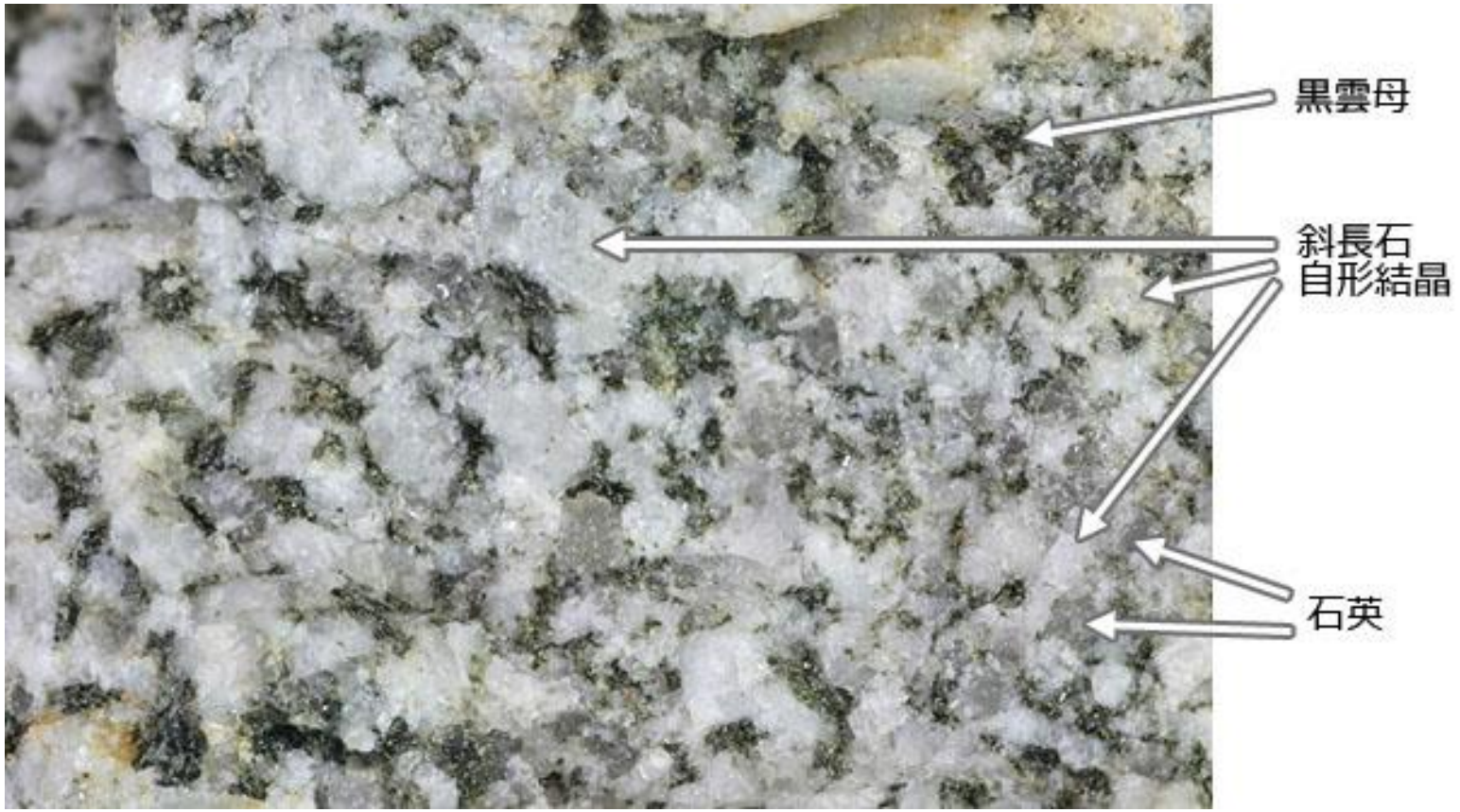


http://www5.plala.or.jp/tepuia/images/samples/trondhjemite_horokanai03_z.jpg

## crosta pós-Arqueana

não ocorre fusão da crosta oceânica subductada

formação de magmas graníticos a granodioríticos

processos de reciclagem crustal

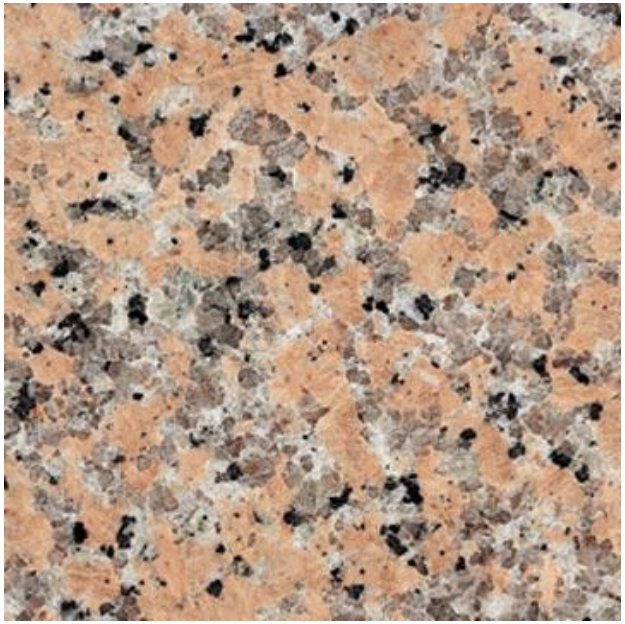

granito

granodiorito

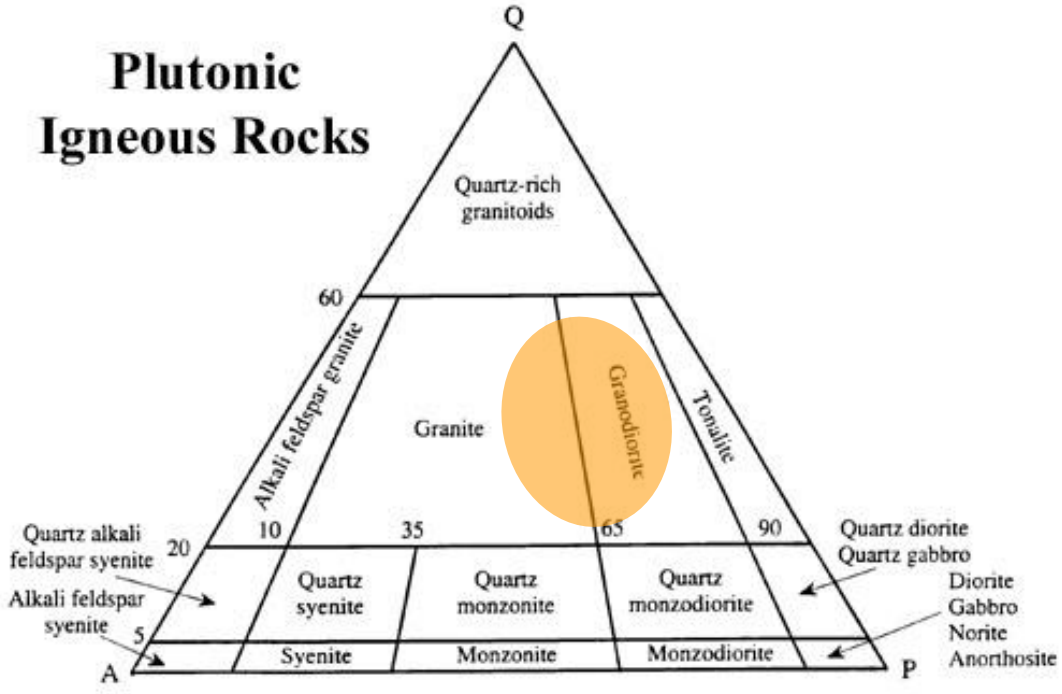

# mais calor interno no Arqueano

Fig. 6.13 The evolution of the Earth's internal heat production since 4.55 Ga. The dashed curve represents the heat resulting from just radioactive decay. Our planet is slowly consuming its store of energy: it progressively cools. (After Brown, 1986.)

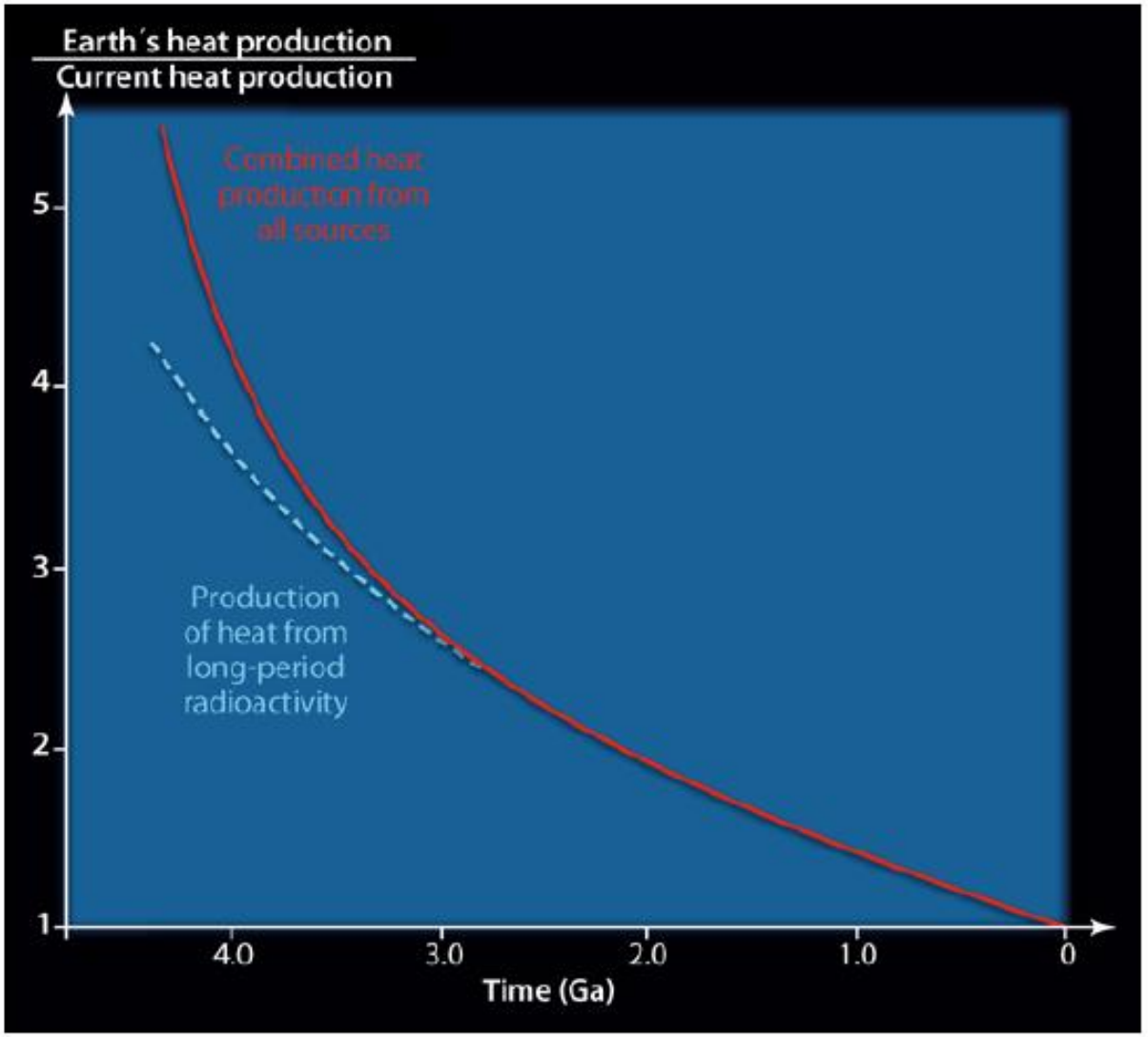

# Arqueano – fusão da crosta oceânica hidradata

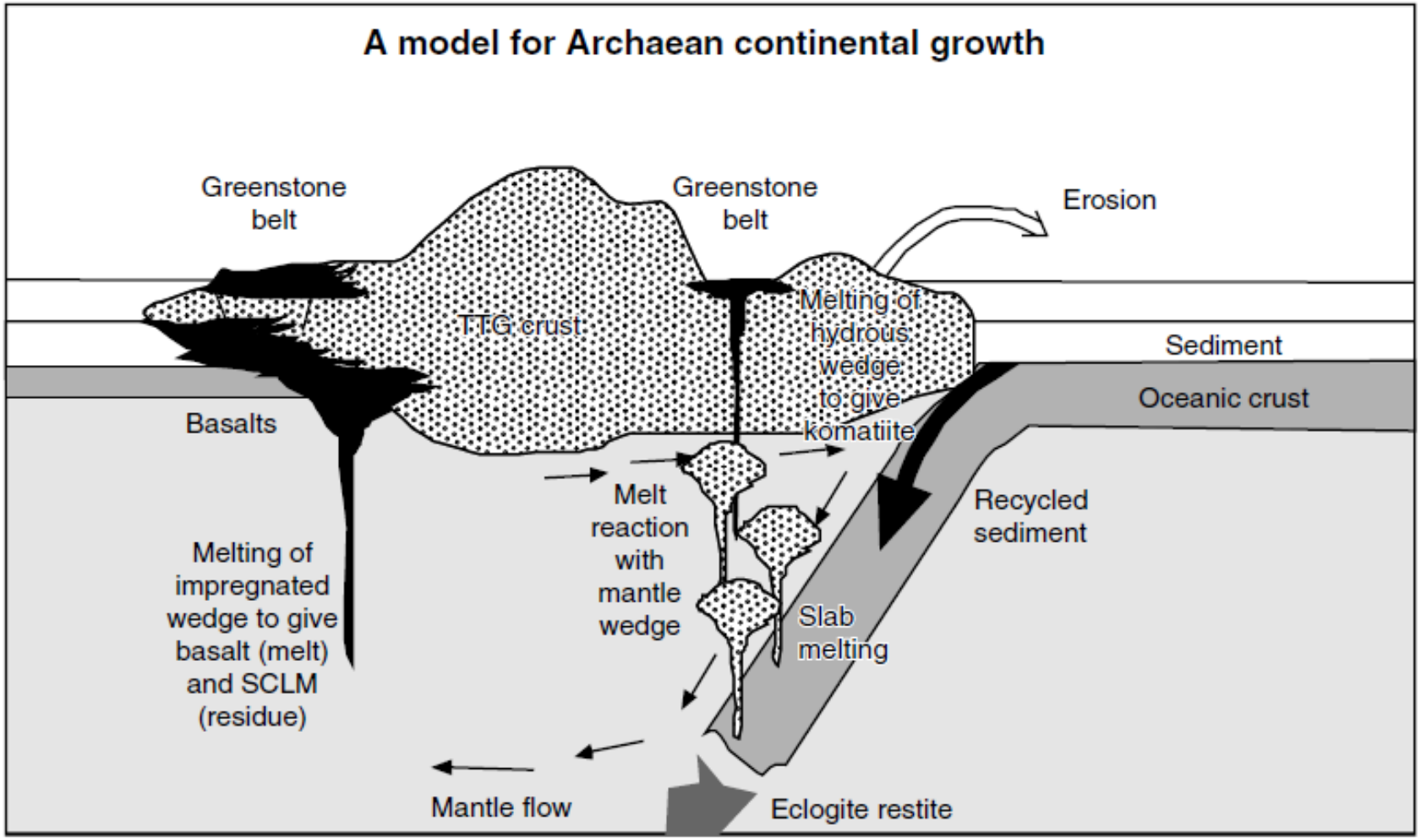


Rollinson, 2007

FIGURE 4.25 A cartoon model indicating the different probable contributions to Archaean continental growth.

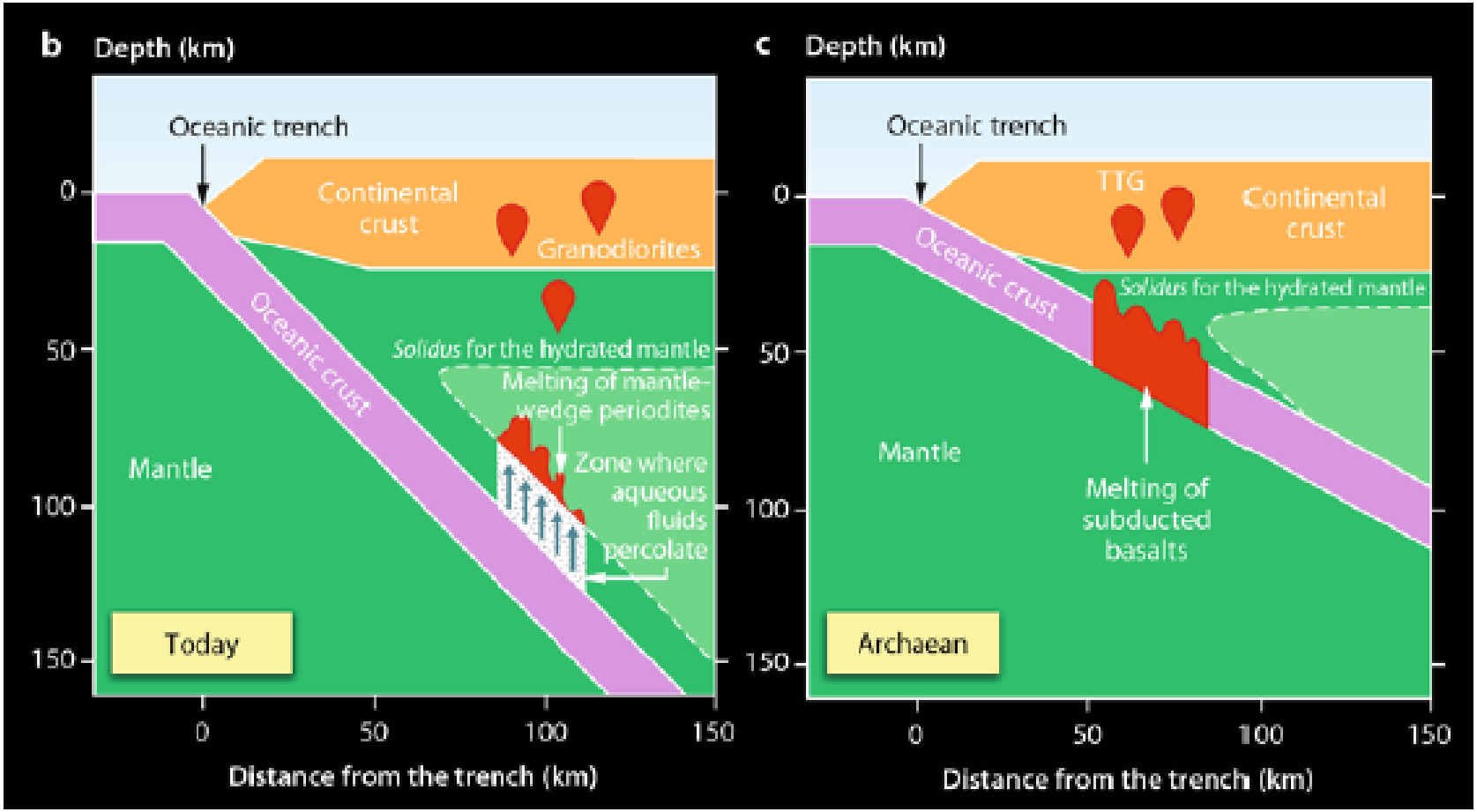


**Fig. 6.12 A pressure (depth) versus temperature diagram (a) and schematic sections of a subduction zone, showing the conditions under which the continental crust has been generated today (b) and during the Archaean (c).** During the Archaean, the geothermal gradients along the Benioff plane were high (pink arrow), such that the subducted oceanic crust reached its *solidus* temperature before it could have been dehydrated. It was therefore able to melt at a relatively shallow depth, in the region where hornblende and garnet are stable (yellow region), giving rise to the TTG magmas, typical of the Archaean continental crust. Today, the geothermal gradients along the Benioff plane are low (blue arrow) and the subducted oceanic crust becomes dehydrated before it can start to melt. The fluids released by the dehydration of the subducted slab ascent through the "mantle wedge", causing its rehydration and metasomatism. While hydrated, the mantle wedge melts and gives rise to calc-alkaline magmas typical of the modern continental crust. The orange and red curves respectively represent the *solidus* for an anhydrous and a hydrated (5% water) basalt. The green curves represent the dehydration reactions that occur in the basalt when hydrous mineral phases are destabilized: (A) = antigorite (serpentine), (C) = chlorite and (T) = talc. The other curves are those for the stability of hornblende (H) and garnet (G). In the schematic sections, the red areas are those where magma is found, and the white area is the region where fluids percolate. (After Martin and Moyen, 2002.)

# rochas do Arqueano

**Table 6.1 Principal characteristics and ages of the oldest crustal remnants known at present.** The TTG (tonalites, trondhjemites and granodiorites) are ancient plutonic rocks whereas the BIF (Banded Iron Formation) and the Nuvvuagittuq gneisses are of sedimentary and volcano-sedimentary origin, respectively. *See also* the classification of rocks on p. 267

| Name | Location | Lithology | Age in Ga |
|---|---|---|---|
| Acasta gneisses | Canada (Northwest Territory) | TTG | 4.031 ± 0.003 |
| Nuvvuagittuq gneisses | Canada (Quebec, Hudson Bay) | Volcano-sedimentary | > 3.825 ± 0.016 |
| Akilia BIF and Isua gneisses | Greenland | BIF | > 3.872 ± 0.010 |
| Amîtsoq gneisses | Greenland | TTG | 3.872 ± 0.010 |
| Uivak gneisses | Canada (Labrador) | TTG | 3.863 ± 0.012 |

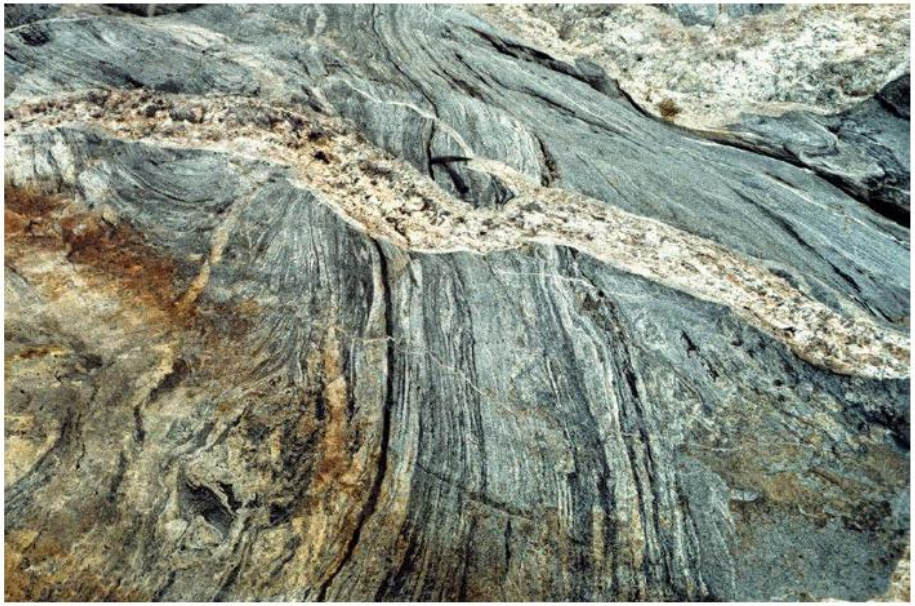

suíte TTG
(trondhjemito, tonalito, granodiorito)

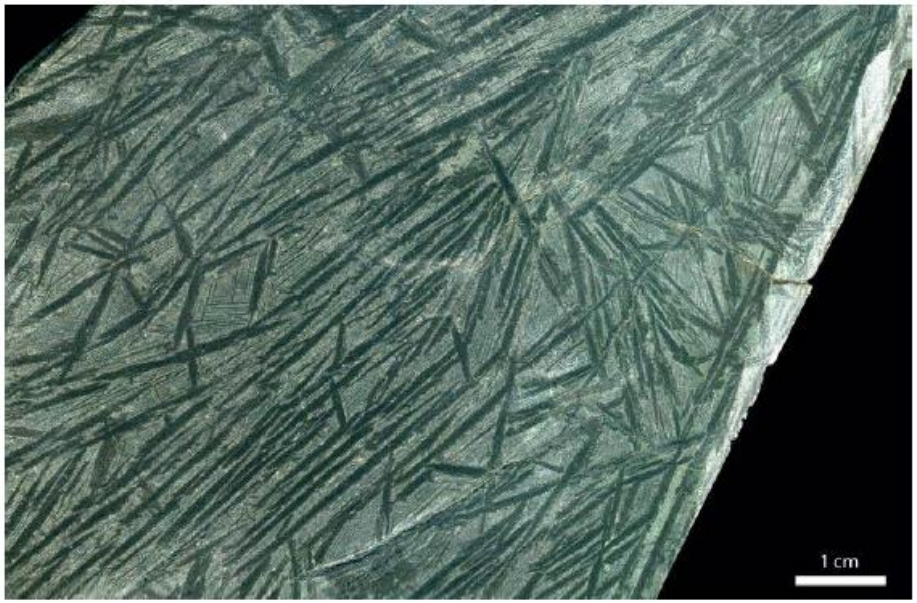


komatiito
(rochas vulcânicas ultramáficas

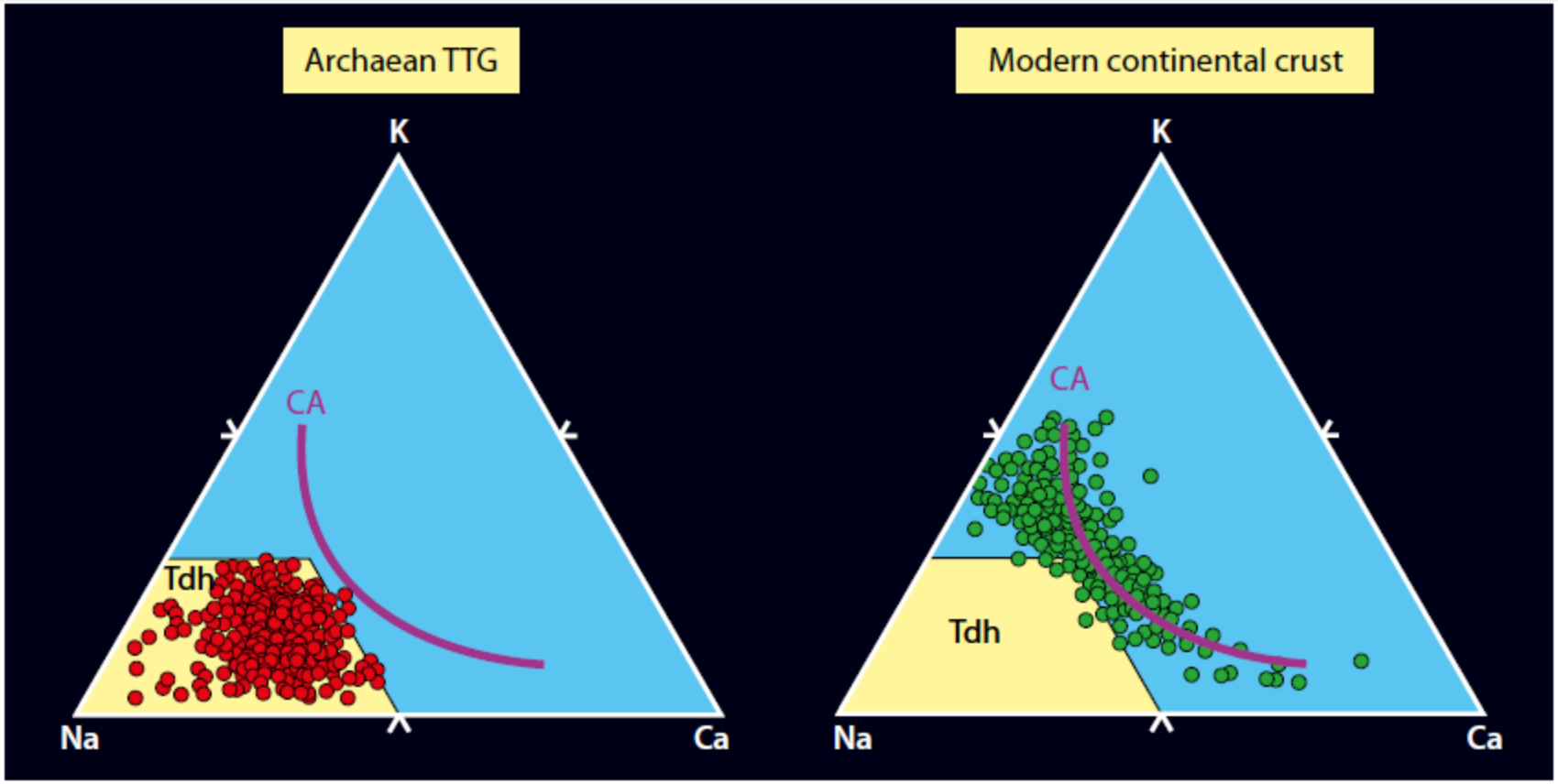


**Fig. 6.11 K-Na-Ca triangle illustrating the differences between Archaean TTGs and the present-day continental crust.** Each apex of the triangle corresponds to a pure pole (100% of the element concerned). The points representing the TTGs plot near the sodium apex in the trondhjemite region (Tdh, pale yellow), whereas their modern equivalents are enriched in potassium and follow a classical calc-alkaline differentiation trend (CA). This shows that the Archaean and modern continental crusts were generated through the melting of different sources, which was a direct consequence of the progressive cooling of our planet. (After Martin, 1995.)

## crosta arqueana


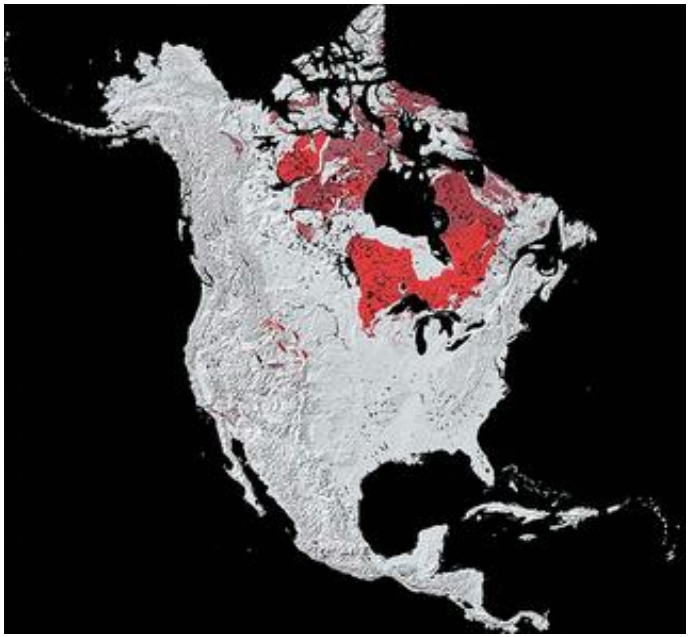

Acasta Gnaisse, Canada, Slave Province

Hadeano 4,03-4,055 Ga

mais antigo fragmento de crosta conhecido

gnaisses tonalíticos, trondjemíticos e granodioríticos suítes TTG

processos que convergem para a formação da crosta continental

diferenciação basalto → andesito

delaminação da crosta inferior

perda preferencial de Mg e Ca dos continentes para os oceanos

formação de crosta félsica no Arqueano  e posterior reciclagem

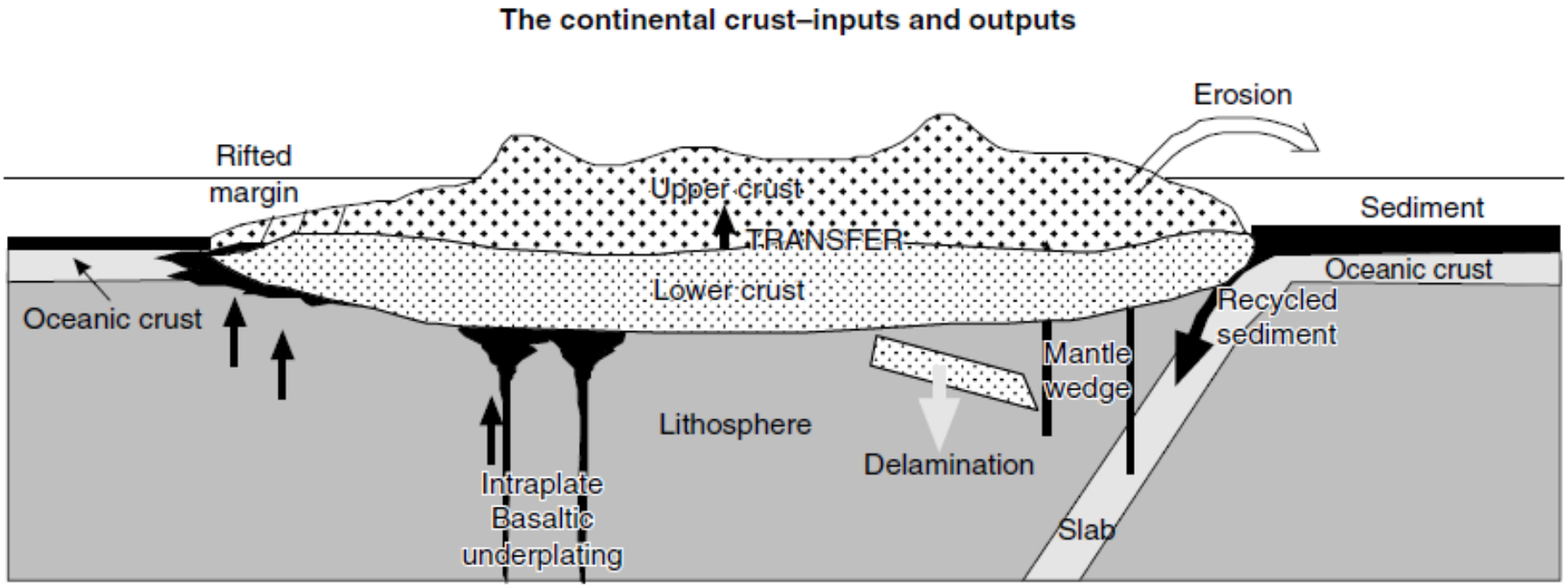


FIGURE 4.5 A model for the fluxes into (black arrows) and out of (white arrows) the continental crust.

Rollinson, 2007

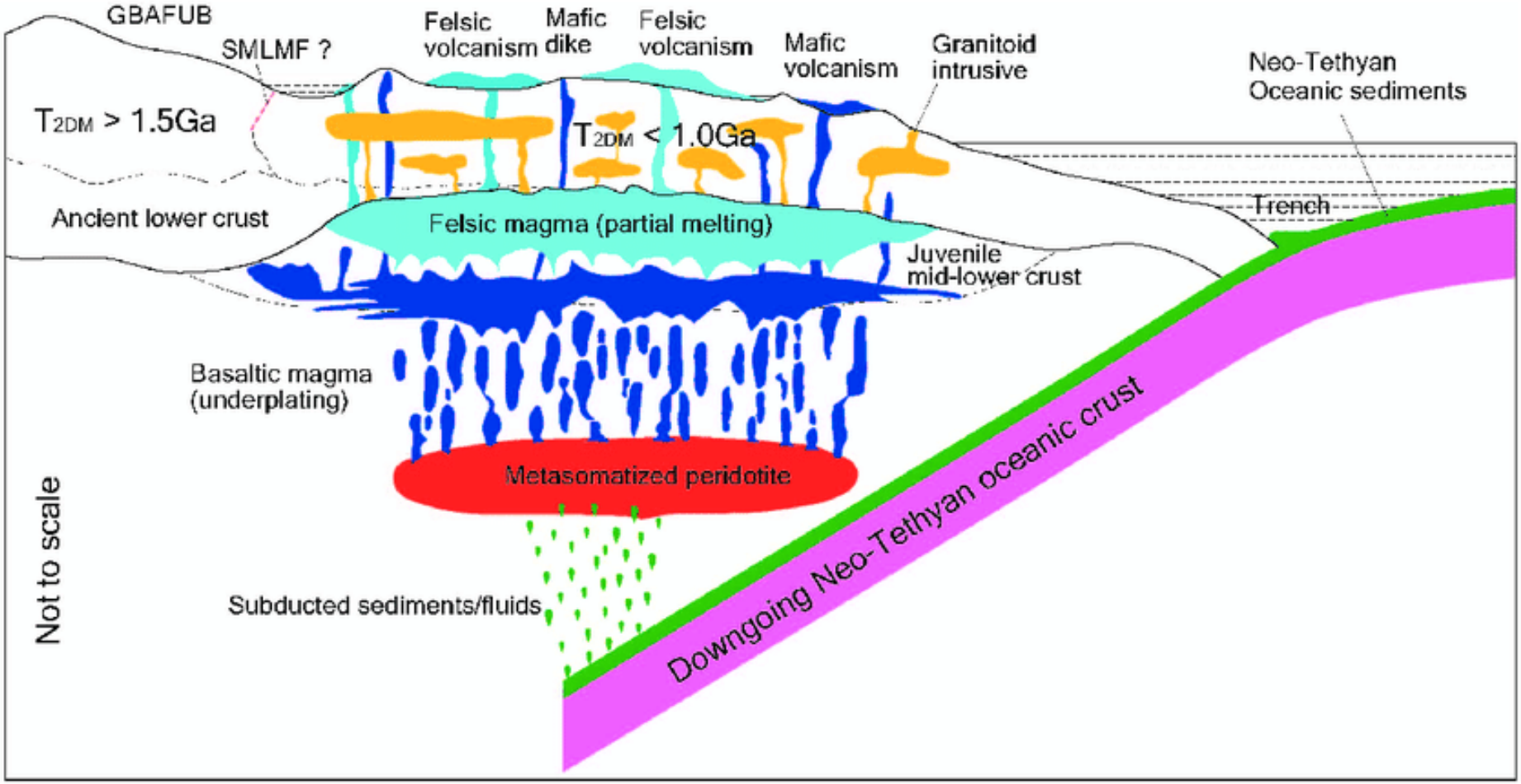


https://www.researchgate.net/publication/249057574_SHRIMP_Zircon_Age_and_Geochemical_Constraints_on_the_Origin_of_Lower_Jurassic_Volcanic_Rocks_from_the_Yeba_Formation_Southern_Gangdese_South_Tibet

# acresção de terrenos

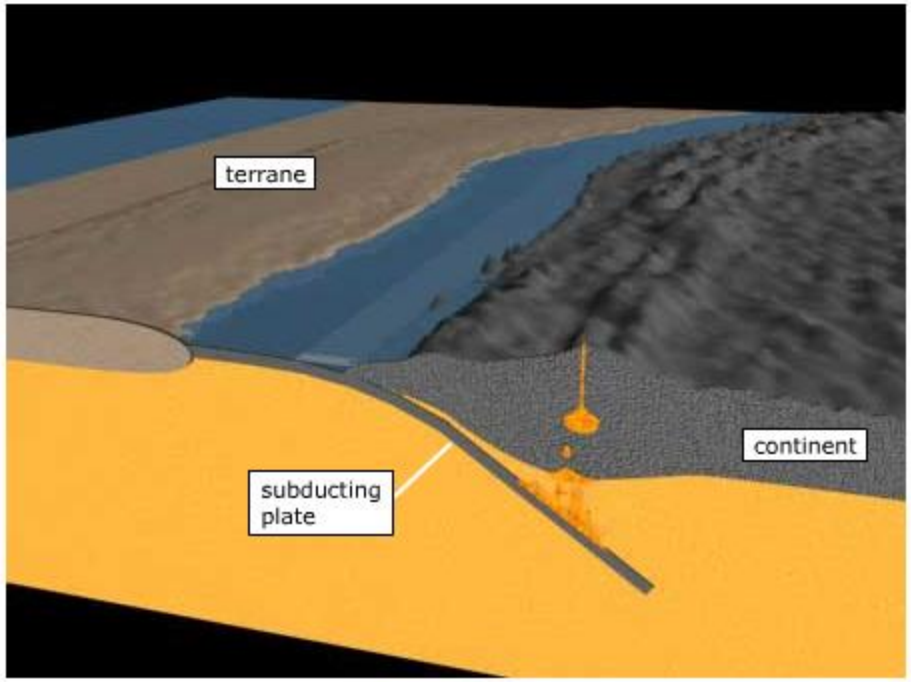


http://www.geology.um.maine.edu/geodynamics/analogwebsite/UndergradProjects2005/Perry/images/terraneaccretionmovie.jpg

# acresção de terrenos

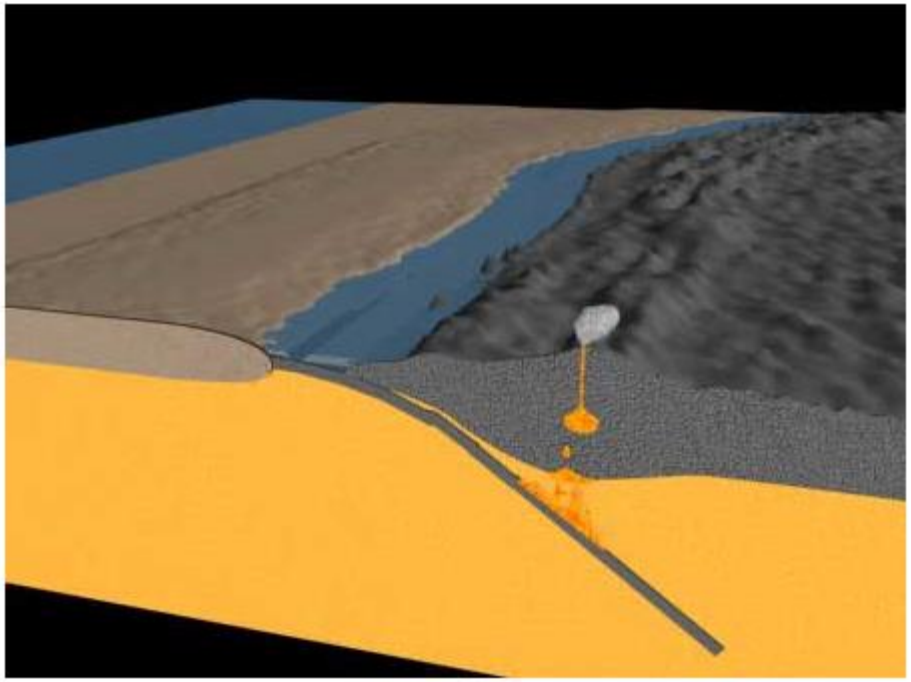

# acresção de terrenos

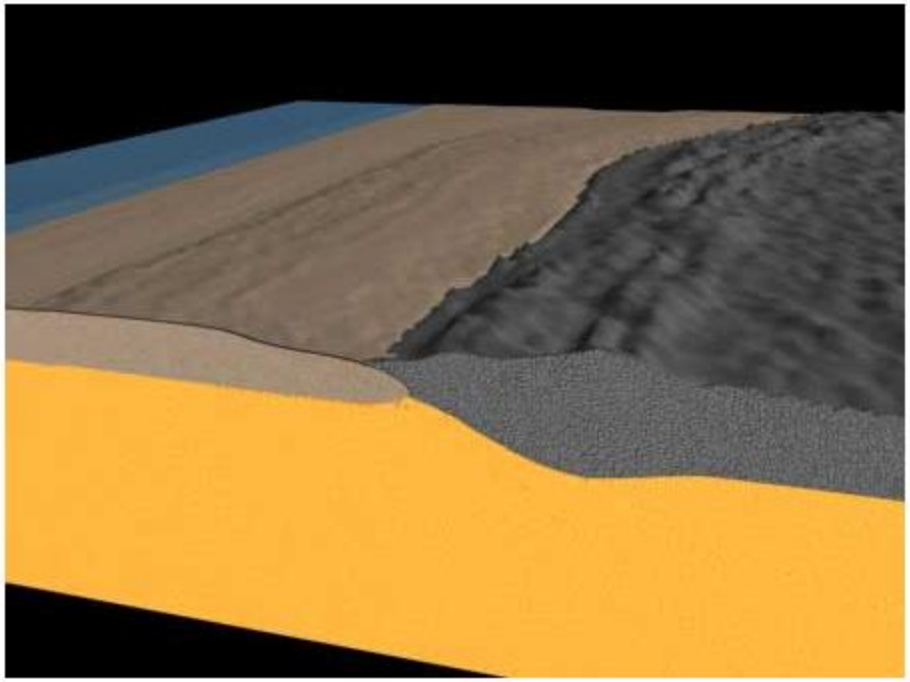

# acresção de terrenos

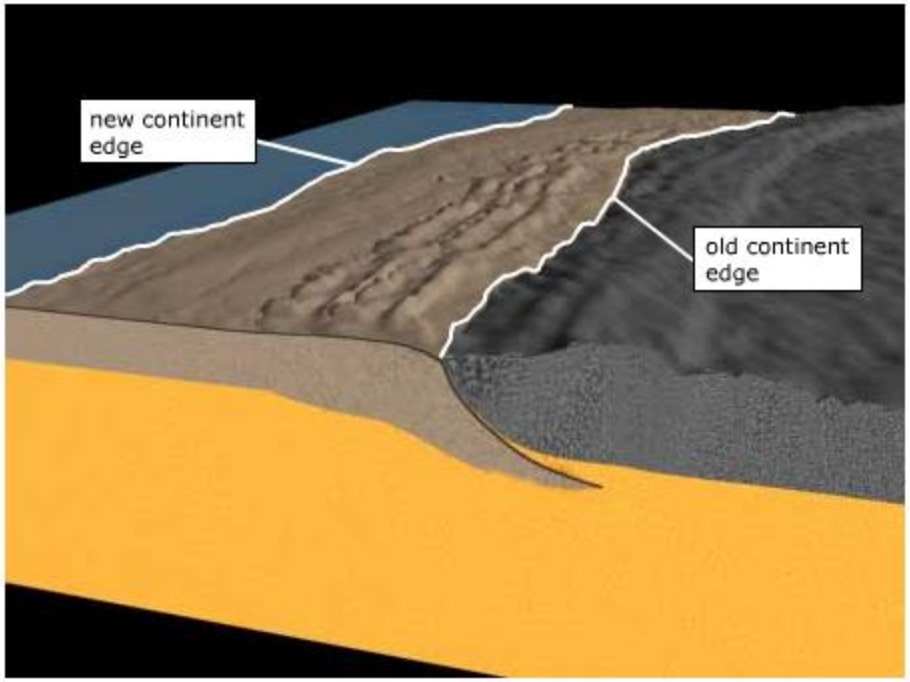

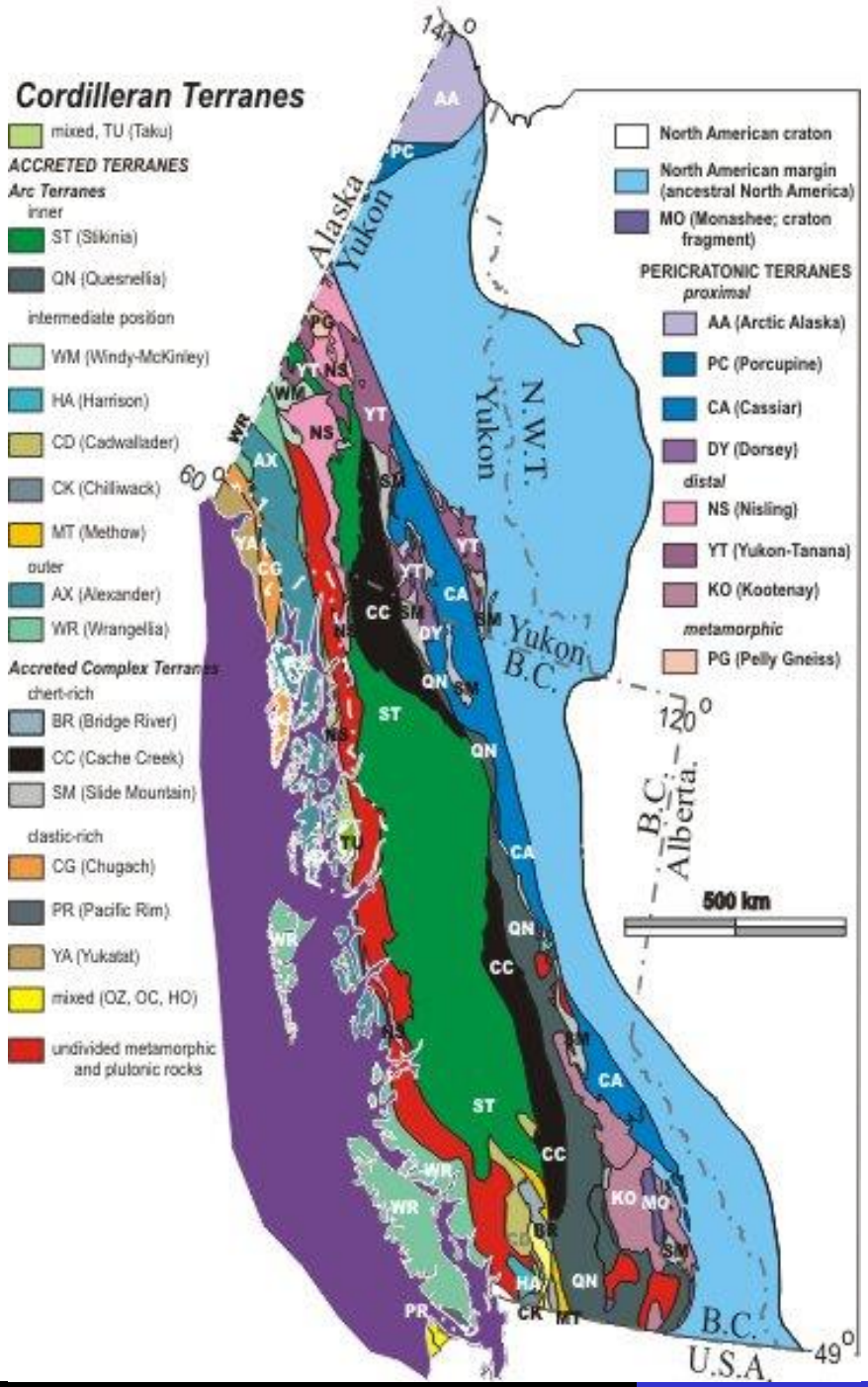


acresção de terrenos

Canadá, costa oeste

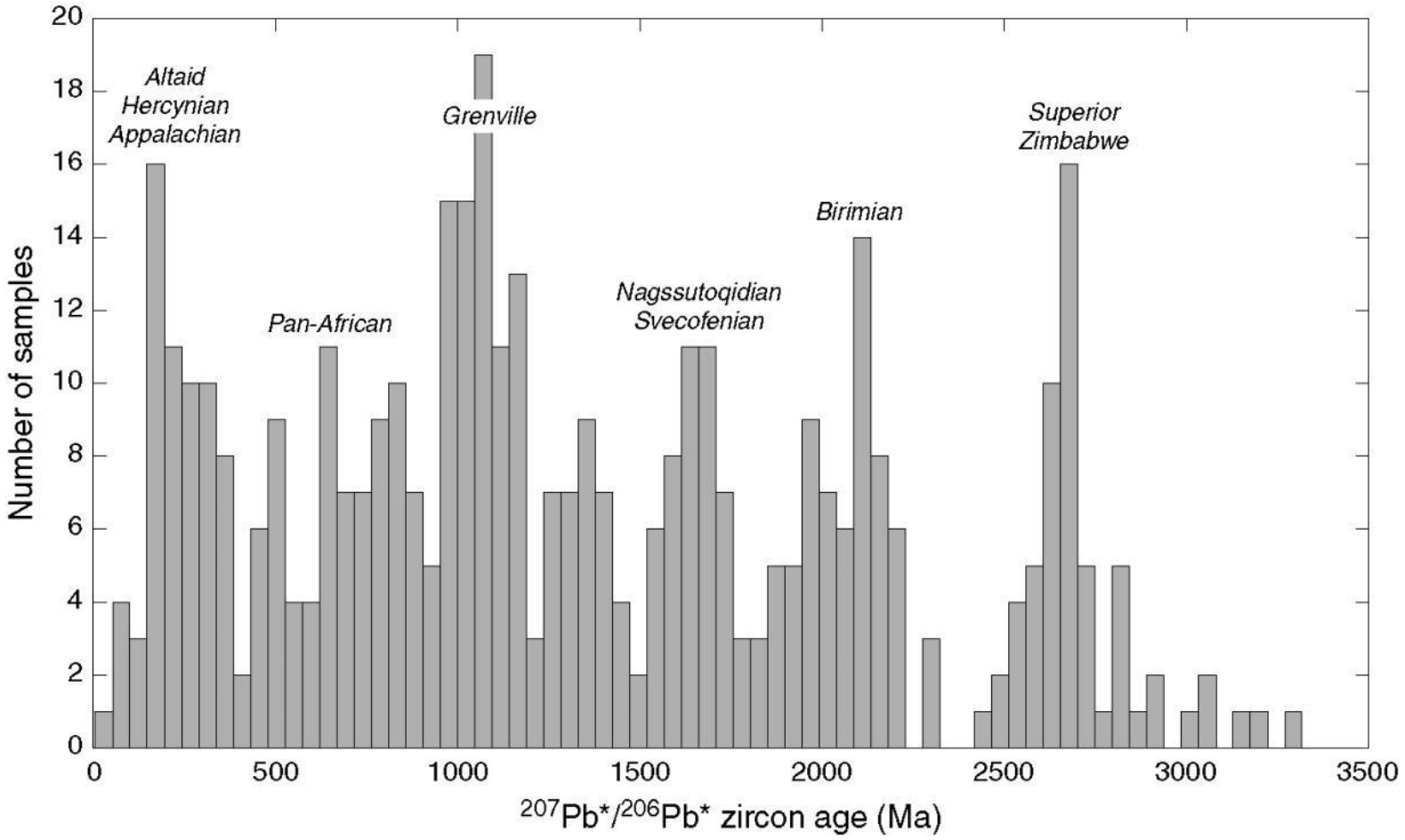


Albarède, 2011

Fig. 11.17 Distribuição de idades U–Pb em cristais de zircão em sedimentos dos quatro maiores rios do mundo, Yangtze, Mississippi, Congo e Amazonas (cortesia de Tsuyoshi Iizuka). Apenas os dados concordades foram considerados no gráfico. Os dados mostram claramente que as rochas graníticas, principais hospedeiras do zircão e representativas da crosta continental, se formaram durante pulsos muito bem definidos. Apenas alguns nomes locais de eventos orogênicos são apresentados.

Geoscience Frontiers 10 (2019) 165–173

HOSTED BY

Contents lists available at ScienceDirect

China University of Geosciences (Beijing)

Geoscience Frontiers

journal homepage: www.elsevier.com/locate/gsf

Research Paper

# Rates of generation and growth of the continental crust

Chris Hawkesworth [a,*], Peter A. Cawood [b], Bruno Dhuime [a,c]

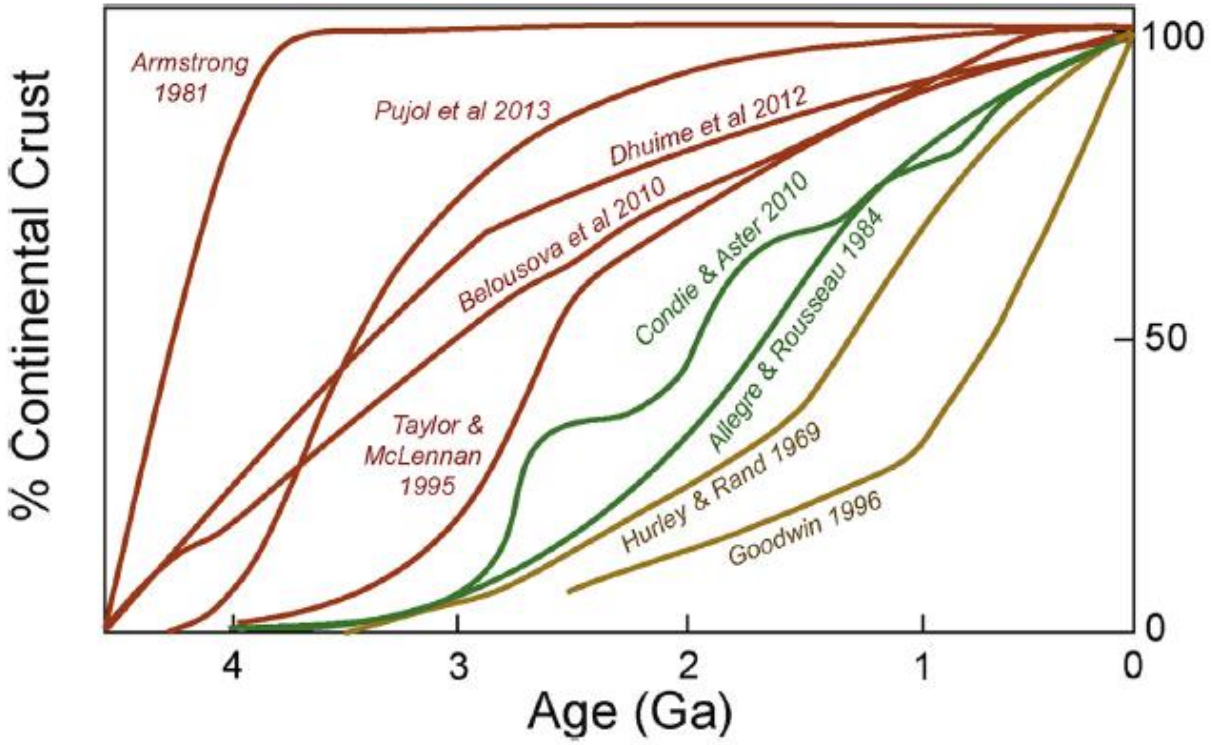


**Figure 5.** Selected crustal growth models. Those in brown are based on the distribution of rocks (Goodwin, 1996), or basement rocks (Hurley and Rand, 1969) of different ages presently preserved on the Earth's surface. The curves in green are based on the assumption that the present day distribution of rocks with different model ages reflects the relative volumes of crust that were present at different times in Earth history (Allègre and Rousseau, 1984; Condie and Aster, 2010). The curves seek to constrain the volumes of crust that were present at different times in Earth history, even if they are no longer preserved at the present day (Armstrong, 1981; Pujol et al., 2013).

# $^{87}Sr/^{86}Sr$ e a diferenciação crosta-manto

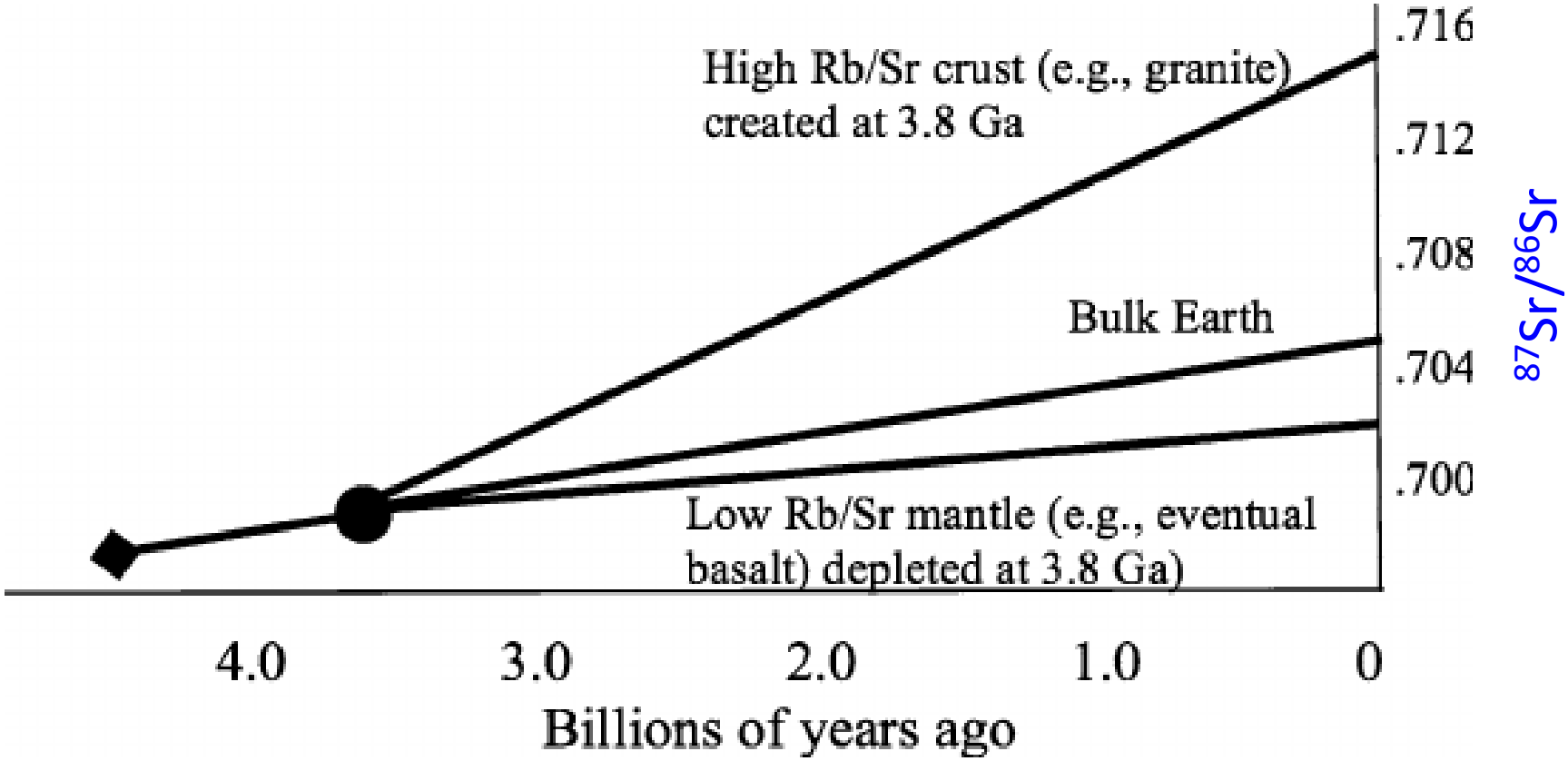

*No water,  no granites – no oceans, no continents* (Campbell e Taylor, 1983)

material terrestre mais antigo

zircão
Jack Hills, 4,404 Ga

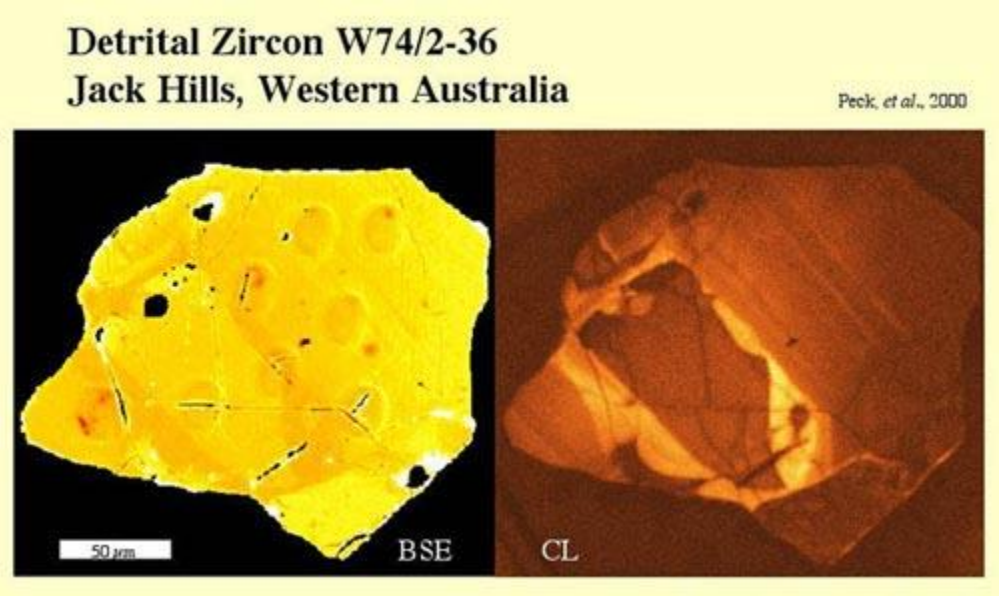


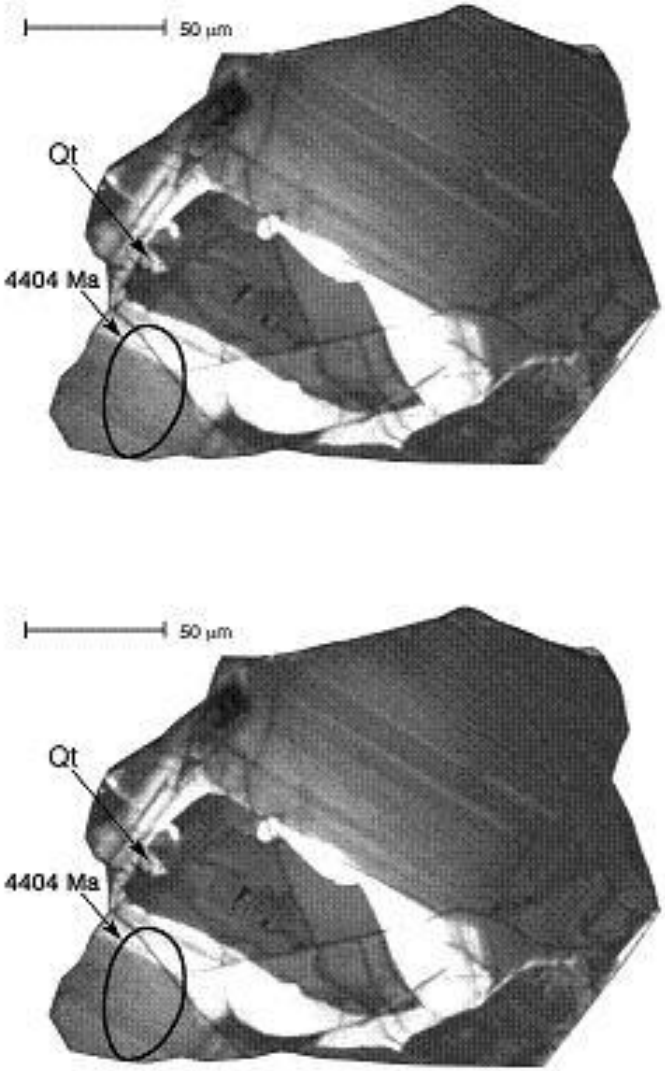

zircões mais antigos da Terra

4,404 Ga

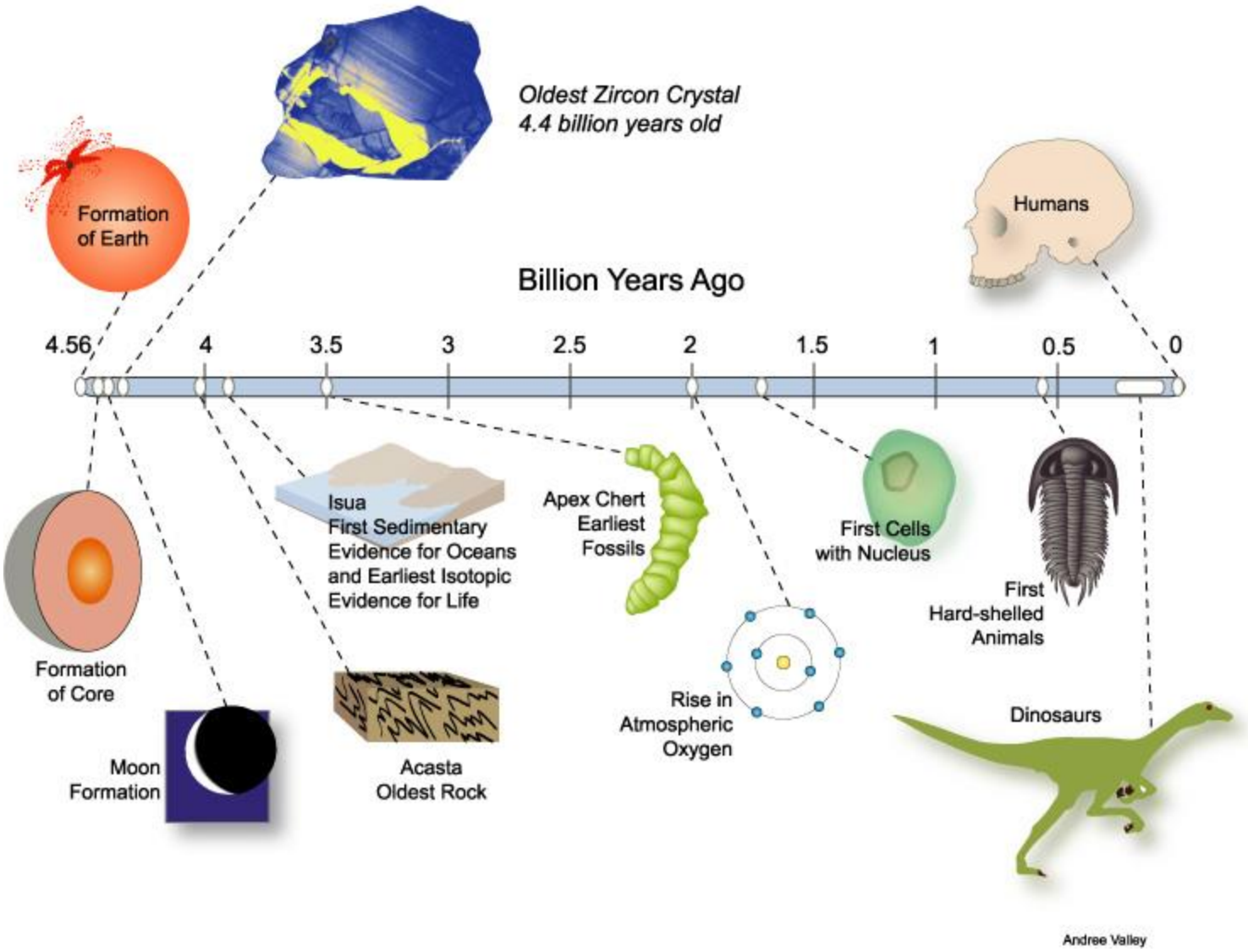

Referências

Young Sun, Early Earth and the Origins of Life, Cap. 6

White, Geochemistry, Cap. 11

Rollinson, Early Earth Systems, 2007. Cap. 4

Albarède, Geoquímica, 2011. Cap. 11

LETTERS
PUBLISHED ONLINE: 22 JUNE 2015 | DOI: 10.1038/NGEO2466
nature geoscience

# Emergence of modern continental crust about 3 billion years ago

Bruno Dhuime[1]*, Andreas Wuestefeld[2] and Chris J. Hawkesworth[1,3]

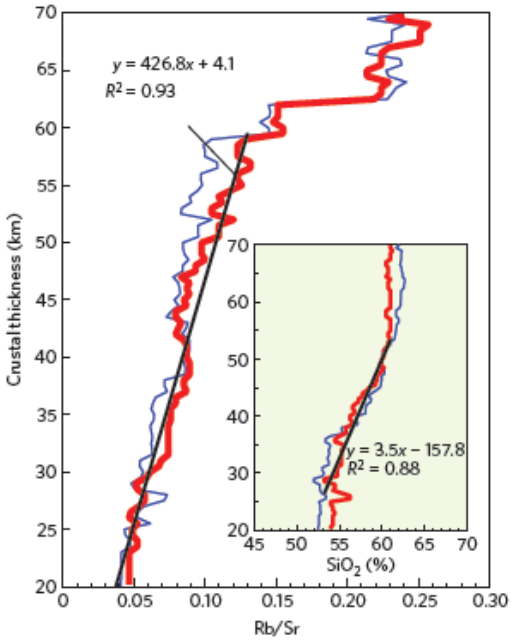


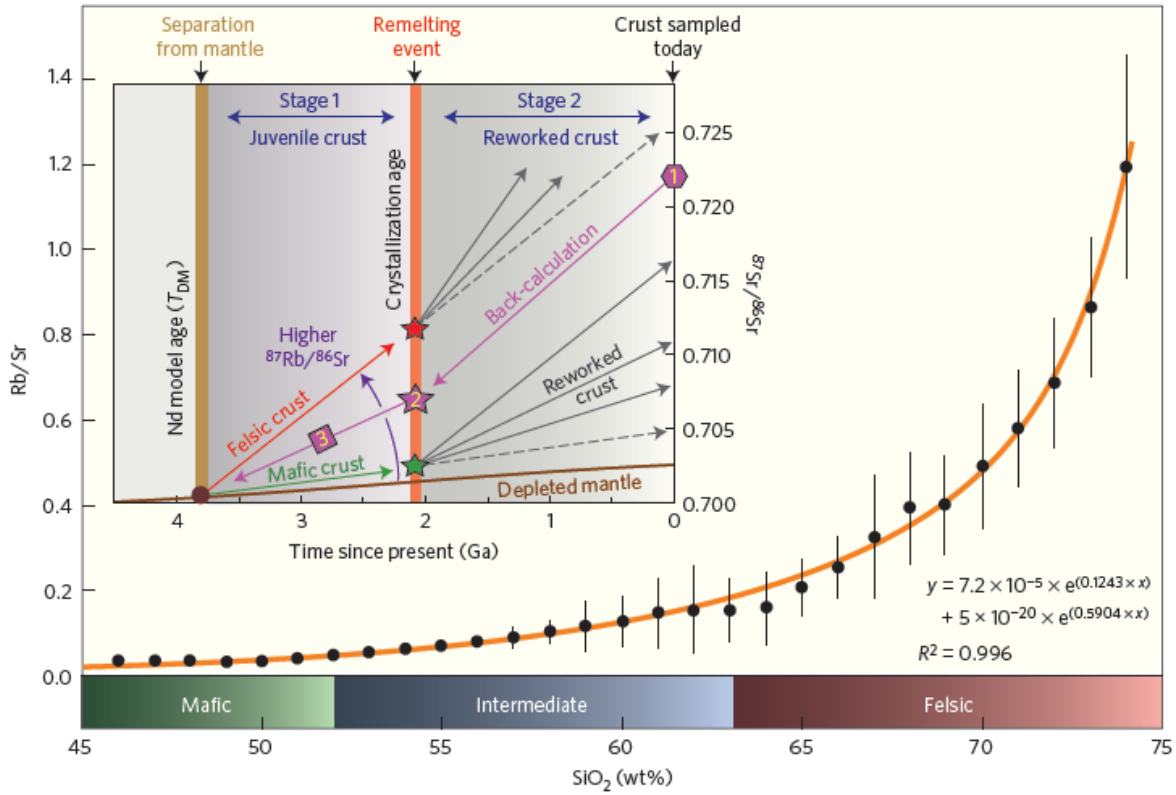


**Figure 1 | Correlation between Rb/Sr and $SiO_2$ in crustal rocks, from a compilation of 96,465 magmatic rocks.** Dots (vertical error bars indicate 2 s.e.m.) represent median Rb/Sr values calculated for each 1% $SiO_2$ interval. The best fit to the data is represented by the orange curve. Inset: Two-stage model of evolution for Sr isotopes used to back-calculate the $^{87}Rb/^{86}Sr$ of the juvenile continental crust (that is, during Stage 1), from Sr–Nd isotopes in the crust sampled today. Purple arrows indicate how the back-calculation was done. Examples for the evolution of a mafic source (green path) and a more felsic source (red path) are presented. Data from GEOROC (http://georoc.mpch-mainz.gwdg.de/georoc).

LETTERS
PUBLISHED ONLINE: 22 JUNE 2015 | DOI: 10.1038/NGEO2466
nature geoscience

# Emergence of modern continental crust about 3 billion years ago

Bruno Dhuime[1]*, Andreas Wuestefeld[2] and Chris J. Hawkesworth[1,3]

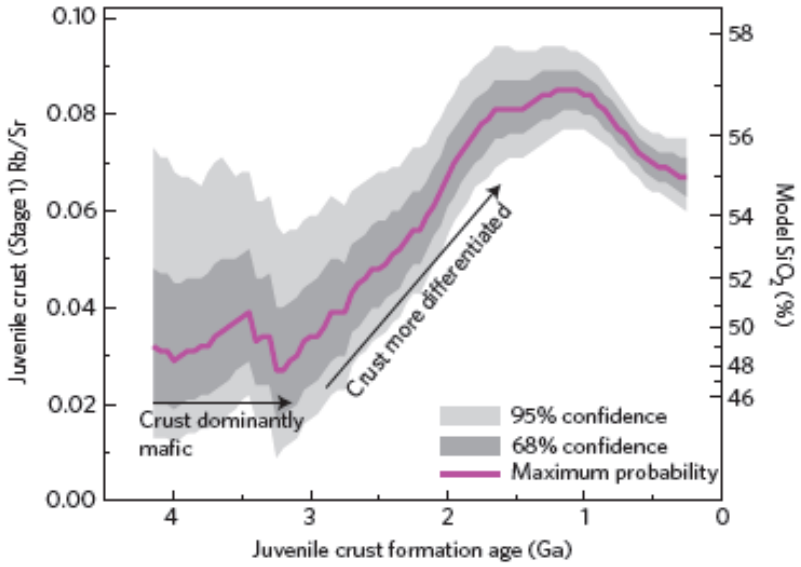


**Figure 2 | Variation of Rb/Sr ratios in juvenile crust (Stage 1 in Fig. 1) as a function its formation age.** Based on a compilation of 13,125 analyses (see Supplementary Dataset 1). Trends in the evolution of Rb/Sr data were determined by employing maximum-likelihood statistics: a gamma distribution was fitted to the histograms of Rb/Sr within sliding windows of 50 Ma widths, and to account for uncertainties in the time axis we used an overlap of 6 windows. The advantage of fitting a probability density function to the data is that we directly obtain a best model fit with associated confidence levels (95% and 68%) for each window. The model $SiO_2$ on the right *y* axis is calculated from the Rb/Sr versus $SiO_2$ relationship in Fig. 1.

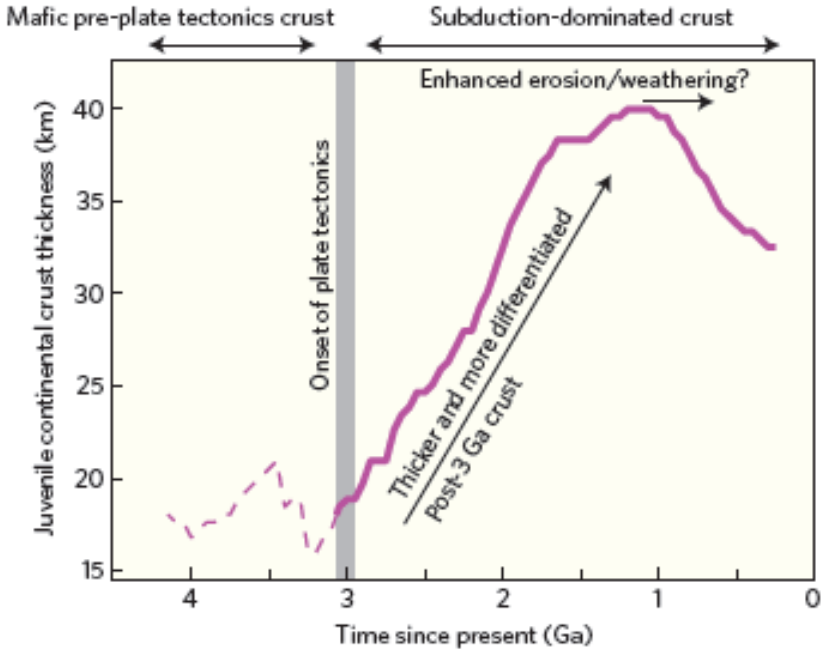


**Figure 4 | Variation in the thickness of juvenile continental crust through time, calculated from the relationships in Figs 2 and 3.** Timing for the onset of plate tectonics is from ref. 5.

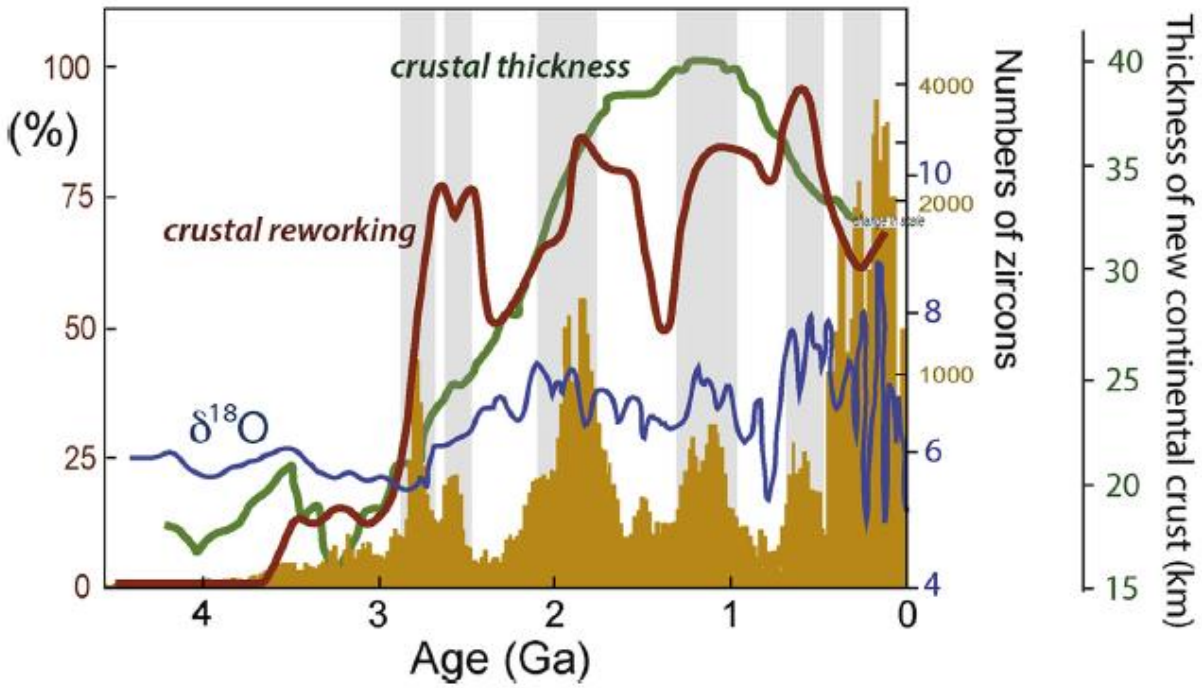


**Figure 8.** A summary of some of the changes that appear to mark the end of the Archaean. These include the development of supercontinents/supercratons, marked by vertical grey bars (Hoffman, 1996; Zhao et al., 2002; Bleeker, 2003; Cawood et al., 2013; Evans, 2013), the increase in the degree of crustal reworking as indicated by Hf isotope ratios in zircon (Belousova et al., 2010; Dhuime et al., 2012), the development of significant peaks in the age distribution of zircons (Campbell and Allen, 2008; Voice et al., 2011), a shift in the composition of juvenile crust from mafic to more intermediate compositions accompanied by an inferred increase in crustal thickness (Dhuime et al., 2015), and the step-up in the $\delta^{18}O$ values in zircons (Valley et al., 2005; Spencer et al., 2014).